ORIGINAL PAPER

Hamid Sharifi (ORCID)

Magneto–thermoelastic behavior of an orthotropic hollow cylinder based on Lord–Shulman and Green–Lindsay theories

Abstract In this research, an analytical solution based on the finite Hankel transformation was developed for the magneto–thermoelasticity problem in an orthotropic hollow cylinder. Two second sound theories of generalized thermoelasticity, the Lord–Shulman and Green–Lindsay theories, were considered in a unified form to study the response of the cylinder subjected to thermal and mechanical loads, as well as a magnetic field. The inner boundary of the cylinder was subjected to a thermal shock in the form of heat flux, while the temperature was kept constant on the outer boundary. The displacement and traction boundary conditions were considered for the inner and outer surfaces of the cylinder, respectively. Closed-from solutions were presented for the magneto–thermoelasticity equations, and effects of the magnetic field intensity on the response of the cylinder were investigated. It was shown that considering finite velocity for the temperature causes propagation and reflection of the thermal wave in the cylinder. The impact of considering orthotropic material properties for the structure was studied, and the results were compared with known data from the literature, revealing strong agreement.

1 Introduction

Cylindrical elements and structures have a broad range of industrial applications. While metals and alloys with isotropic material properties are widely utilized to manufacture mechanical components, new manufacturing processes may change the mechanical properties of the materials during the process. For instance, parts created using metal additive manufacturing experience complex thermal loads, potentially resulting in anisotropic material properties which differ from those of parts manufactured using traditional methods [1]. Therefore, investigating the effects of anisotropic material properties for the mechanical components appears to be a crucial factor in the design process.

In classical thermoelasticity, which was developed based on Fourier's heat conduction law, the second derivative of temperature with respect to time does not exist, and the absence of this term in the heat conduction equation implies that the temperature wave travels at infinite speed. While classical thermoelasticity can successfully predict stress distribution for a wide range of engineering problems, its results deviate from actual physical behavior of materials at temperatures near zero Kelvin or when subjected to thermal shocks [2]. To address this problem and present more accurate predictions, second sound theories of thermoelasticity such as Lord–Shulman and Green–Lindsay were proposed [3].

Typically, structures in real-world applications are subjected to various types of loads, such as thermal or mechanical shocks, magnetic or electrical fields, or combination of these loads. For example, magneto–electro–elastic composites have various applications in energy harvesting, actuators and sensing devices [4]. In

H. Sharifi (✉)
College of Engineering and Science, Louisiana Tech University, P.O.B. 71272, Ruston, LA, USA
e-mail: hsh012@latech.edu

addition, a wide range of materials exhibit anisotropic properties. Taking this into account, solving the magneto–thermoelasticity problem in anisotropic media, such as cylinders, has emerged as a topic of significant interest. In this regard, Sherief and Ezzat [5] used Fourier series expansion to solve the problem of generalized magneto–thermoelasticity in a long annular cylinder based on the Lord–Shulman theory. Zenkour and Abbas [6] investigated the magneto–thermoelastic response of a functionally graded hollow cylinder using the finite element method, and Hosseini and Dini [7] presented an analytical solution for the same problem in a rotating functionally graded thick cylinder. Abd-El-Salam et al. [8] used finite difference method to address the magneto–thermoelasticity problem in a non-homogeneous isotropic cylinder based on the hyperbolic heat conduction equation. Das et al. [9] studied the magneto–thermoelastic response of a transversely isotropic hollow cylinder subjected to a thermal shock using the Green–Naghdi type III thermoelasticity. The Laplace transform and the Galerkin finite element method were used to solve the governing equations. Abbas [10] developed the equations of generalized magneto–thermoelasticity in a nonhomogeneous hollow cylinder based on the Green–Lindsay and Lord–Shulman theories. In a separate study, the same author [11] used the Lord–Shulman theory to investigate the magneto–thermoelastic interaction in a fiber–reinforced transversely isotropic hollow cylinder. Abd-Alla and Mahmoud [12] used implicit finite difference method to study magneto–thermoelasticity of a rotating non-homogeneous orthotropic hollow cylinder, using the hyperbolic heat conduction equation with one relaxation time. They also investigated the effects of rotation, inhomogeneity, and magnetic field on the response of the cylinder. Biswas [13] employed the three–phase lag generalized thermoelasticity and the eigenvalue approach to investigate the magneto–thermoelasticity problem in a transversely isotropic hollow cylinder. Othman and Abbas [14] employed the finite element method and the Green–Naghdi theory of type III to investigate the influence of rotation on the magneto–thermoelastic response of a homogeneous isotropic hollow cylinder with energy dissipation. Said et al. [15] utilized the two-temperature fractional-order thermoelasticity to study the effects of the magnetic field on the stress distribution of a rotating thick hollow cylinder using the harmonic wave technique. Ezzat and El-Bary [16] employed the Laplace transform to analyze impacts of variable thermal conductivity on the stress and temperature distribution in a long hollow cylinder, using generalized magneto–thermoelasticity based on fractional order heat conduction. Sherief and Allam [17] studied 2-D electro–magneto interaction in an infinitely long solid cylinder using generalized electro–magneto–thermoelasticity with one relaxation time and employing the Laplace transform and the potential functions. Patra et al. [18] employed finite difference method to study the magneto–thermoelastic response of a nonhomogeneous isotropic rotating hollow cylinder, based on the Lord–Shulman and Green–Lindsay theories. Akbarzadeh and Chen [19] presented an exact solution for thermo–magneto–electro–elastic responses of rotating hollow cylinders. The problem had the steady state conditions, and both functionally graded and homogeneous orthotropic material properties were considered for the cylinders. Othman studied the electro—magneto–thermos–elastic behavior of an elastic half-space using different theories of thermoelasticity [20–22]. Othman and Abd-Elaziz [23] investigated the effect of rotation and gravitational field on a micropolar magneto–thermoelastic solid using the dual-phase lag model. Additionally, Othman et al. [24] employed five different theories of thermoelasticity to study the effects of the magnetic field on the thermoelastic behavior of a rotating medium.

In the context of the analytical solutions, due to the complicated equations of generalized thermoelasticity, many approaches were developed based on classical thermoelasticity, owing to the complexity of the generalized thermoelasticity equations. In cylindrical coordinates, different problems involving both homogenous and nonhomogeneous materials were solved [25–30]. Bagri and Eslami utilized the Galerkin finite element method to solve the Lord–Shulman generalized thermoelasticity in isotropic [31] and functionally graded disks [32]. The same problem for an orthotropic rotating disk was solved by Sharifi [33]. Kiani and Eslami [34] used the Generalized Differential Quadrature (GDQ) method to investigate thermally nonlinear generalized thermoelasticity in disks, and Kiani and Zeverdejani [35] employed the same method to address a similar problem for an exponentially graded disk. Tokovyy et al. [36] presented an analytical solution for the axisymmetric thermoelasticity problem in a long solid cylinder with varying thermomechanical properties.

Bagri and Eslami [37] proposed a new unified formulation that included the Lord–Shulman, Green–Lindsay and Green–Naghdi theories of generalized thermoelasticity. Sharifi [38] used a unified formulation of generalized thermoelasticity, incorporating both the Lord–Shulman and Green–Lindsay theories to study the dynamic response of an orthotropic hollow cylinder under thermal shock. The same problem in an orthotropic hollow sphere investigated by Soroush and Soroush [39]. Othman and Abbas [40] studied the generalized thermoelasticity of a non-homogeneous isotropic hollow cylinder based on the Green–Naghdi theory of type II and III. Tiwari and Abouelregal [41] employed fractional-order Kelvin–Voigt thermoelasticity with three-phase lag to investigate the behavior of a viscoelastic transversely isotropic rotating hollow cylinder under
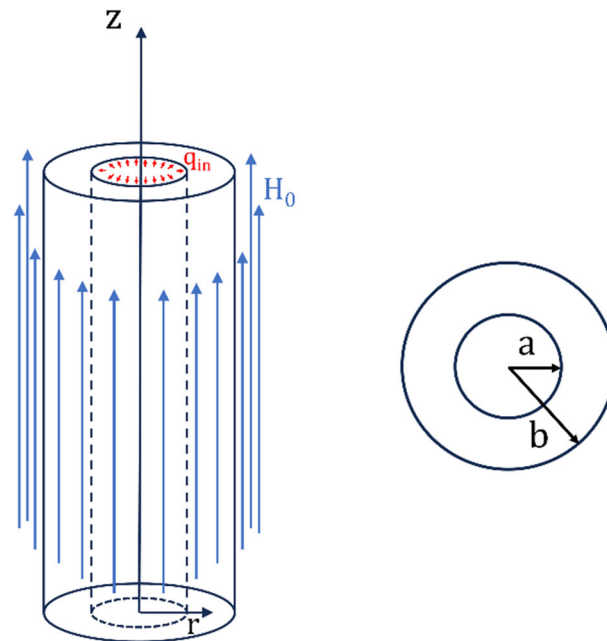
Fig. 1 Geometry of the problem

a thermal load and a magnetic field. The problem was solved using the Laplace transform and the effects of considering elastic and viscoelastic materials were studied. Additionally, other types of materials, such as porothermoelastic [42] and Cosserat media [43], were investigated using different thermoelasticity theories.

To the best knowledge of the author, the problem of generalized magneto–thermoelasticity in orthotropic cylinders based on the Lord–Shulman and Green–Lindsay theories has not been solved analytically yet. In this research, an orthotropic hollow cylinder subjected to mechanical and thermal loads, as well as a magnetic field, was considered and the equations of generalized magneto–thermoelasticity based on the Lord–Shulman and Green–Lindsay theories were extracted, and the closed-form solutions were presented. Subsequently, the problem of an orthotropic hollow cylinder subjected to a thermal shock in the form of heat flux on its inner surface was investigated. Numerical results for different scenarios, including the effects of magnetic field intensity and orthotropic material properties on the history and distribution of the stress components, were illustrated in the figures. To validate the results of the presented solution, the special case of generalized thermoelasticity based on the Lord–Shulman theory in an isotropic disk subjected to a thermal shock was considered, and the history of temperature, displacement, the radial and hoop stress components were compared with the results presented by Kiani and Eslami [34], showing a good agreement.

2 Governing equations

Consider an orthotropic cylinder with the inner and outer radii a and b, which is subjected to axisymmetric thermal and mechanical loadings. The geometry of the problem is shown in Fig. 1.

Due to the symmetry in the boundary conditions and the geometry of the problem, the displacement components in the circumferential and axial directions are zero, and the temperature and displacement distributions at each point depend only on the radial position. Previously, unified equations of the generalized thermoelasticity for this problem were presented in the following form [38]:

$$k\left(\frac{\partial^2\theta}{\partial r^2} + \frac{1}{r}\frac{\partial\theta}{\partial r}\right) - \rho c\frac{\partial\theta}{\partial t} - \rho c t_2\frac{\partial^2\theta}{\partial t^2} - T_0\beta_{11}\left(\frac{\partial\dot{u}}{\partial r} + t_3\frac{\partial\ddot{u}}{\partial r}\right) - T_0\beta_{22}\left(\frac{\dot{u}}{r} + t_3\frac{\ddot{u}}{r}\right) = 0 \tag{1}$$

$$c_{11}\left(\frac{\partial^2 u}{\partial r^2} + \frac{1}{r}\frac{\partial u}{\partial r}\right) - c_{22}\frac{u}{r^2} - \beta_{11}\left(\frac{\partial\theta}{\partial r} + t_1\frac{\partial\dot{\theta}}{\partial r}\right) - \frac{1}{r}(\beta_{11} - \beta_{22})[\theta + t_1\dot{\theta}] + F_r = \rho\ddot{u} \tag{2}$$

where k is the thermal conduction coefficient in radial direction, ρ is the density, c is heat capacity, c_{ij} are the elastic constants and are defined as below:

$$c_{11} = \frac{(1 - \nu_{23}\nu_{32})}{1 - \nu_t} E_1, \quad c_{12} = \frac{(\nu_{21} + \nu_{31}\nu_{23})}{1 - \nu_t} E_1,$$
$$c_{22} = \frac{(1 - \nu_{13}\nu_{31})}{1 - \nu_t} E_2, \quad c_{13} = \frac{(\nu_{31} + \nu_{21}\nu_{32})}{1 - \nu_t} E_1,$$
$$c_{33} = \frac{(1 - \nu_{12}\nu_{21})}{1 - \nu_t} E_3, \quad c_{23} = \frac{(\nu_{32} + \nu_{12}\nu_{31})}{1 - \nu_t} E_2,$$
$$c_{44} = G_{23}, \ c_{55} = G_{13}, \ c_{66} = G_{12}, \tag{3}$$

$$\nu_t = \nu_{12}\nu_{21} + \nu_{23}\nu_{32} + \nu_{13}\nu_{31} + \nu_{12}\nu_{23}\nu_{31} + \nu_{21}\nu_{32}\nu_{13} \tag{4}$$

ν_{ij} and E_i are Poisson's ratios and Young's moduli in different directions where 1, 2 and 3 correspond with r, φ and z directions, respectively. Also, we have:

$$\beta_{11} = c_{11}\alpha_r + c_{12}\alpha_\varphi + c_{13}\alpha_z \tag{5}$$

$$\beta_{22} = c_{12}\alpha_r + c_{22}\alpha_\varphi + c_{23}\alpha_z \tag{6}$$

$$\beta_{33} = c_{13}\alpha_r + c_{23}\alpha_\varphi + c_{33}\alpha_z \tag{7}$$

Equations (1) and (2) comprise both Lord–Shulman and Green–Lindsay theories of thermoelasticity. These equations reduce to the Lord–Shulman theory when $t_1 = 0$ and $t_2 = t_3$, and if $t_3 = 0$, the equations of the Green–Lindsay theory can be obtained. Additionally, the relationship between stress and strain components for orthotropic material properties in the polar coordinates (when $t_1 = 0$) can be found in different references such as [44]:

$$\begin{bmatrix} \sigma_{rr} \\ \sigma_{\varphi\varphi} \\ \sigma_{zz} \\ \tau_{\varphi z} \\ \tau_{rz} \\ \tau_{r\varphi} \end{bmatrix} = \begin{bmatrix} c_{11} & c_{12} & c_{13} & 0 & 0 & 0 \\ c_{12} & c_{22} & c_{23} & 0 & 0 & 0 \\ c_{13} & c_{23} & c_{33} & 0 & 0 & 0 \\ 0 & 0 & 0 & c_{44} & 0 & 0 \\ 0 & 0 & 0 & 0 & c_{55} & 0 \\ 0 & 0 & 0 & 0 & 0 & c_{66} \end{bmatrix} \begin{bmatrix} \varepsilon_{rr} - \alpha_r \Delta T \\ \varepsilon_{\varphi\varphi} - \alpha_\varphi \Delta T \\ \varepsilon_{zz} - \alpha_z \Delta T \\ \gamma_{\varphi z} \\ \gamma_{rz} \\ \gamma_{r\varphi} \end{bmatrix} \tag{8}$$

where ΔT is the temperature variation, α_r, α_φ and α_z are thermal expansion coefficients in three main directions of the cylinder. Also, we have:

$$\theta = T(r, t) - T_0 \tag{9}$$

T_0 is the reference temperature of the orthotropic cylinder. By considering axisymmetric boundary conditions for the problem, all stress components become zero except σ_{rr} and $\sigma_{\varphi\varphi}$. The strain components can be expressed as a function of the radial displacement u as follows:

$$\varepsilon_{rr} = \frac{\partial u}{\partial r}, \varepsilon_{\varphi\varphi} = \frac{u}{r}, \varepsilon_{\varphi z} = \varepsilon_{zr} = \varepsilon_{r\varphi} = 0 \tag{10}$$

In addition, the radial stress (σ_{rr}) and hoop stress ($\sigma_{\theta\theta}$) components are functions of the radial displacement and the temperature, and can be obtained in the following form [3, 45]:

$$\sigma_{rr} = c_{11}\frac{\partial u}{\partial r} + c_{12}\frac{u}{r} - \beta_{11}(\theta + t_1\dot{\theta}) \tag{11}$$

$$\sigma_{\varphi\varphi} = c_{12}\frac{\partial u}{\partial r} + c_{22}\frac{u}{r} - \beta_{22}(\theta + t_1\dot{\theta}) \tag{12}$$

Now consider the orthotropic hollow cylinder is subjected to a constant magnetic field in the Z direction with H_0 intensity, which induces a magnetic field $\vec{h}$ and an electric field $\vec{E}$. With slow movement of the

cylinder in the magnetic field, the Lorentz force is applied to the cylinder. The equation of this force in polar coordinate was presented by Karimipour Dehkordi1and Kiani [46]:

$$F_r = \mu_0 H_0^2 \left(\frac{\partial^2 u}{\partial r^2} + \frac{1}{r} \frac{\partial u}{\partial r} - \frac{u}{r^2} - \varepsilon_0 \mu_0 \ddot{u} \right) \tag{13}$$

where ε_0 and μ_0 are electric permittivity and magnetic permeability, respectively, and induced magnetic and electric fields can be calculated using the following formulas [46]:

$$E_0 = \mu_0 H_0 \dot{u} \tag{14}$$

$$h_0 = -H_0 \left(\frac{u}{r} + \frac{\partial u}{\partial r} \right) \tag{15}$$

By inserting Eq. (13) into Eqs. (1) and (2), the equations of the generalized magneto–thermoelasticity in an orthotropic hollow cylinder can be expressed in the following form:

$$k \left(\frac{\partial^2 \theta}{\partial r^2} + \frac{1}{r} \frac{\partial \theta}{\partial r} \right) - \rho c \frac{\partial \theta}{\partial t} - \rho c t_2 \frac{\partial^2 \theta}{\partial t^2} - T_0 \beta_{11} \left(\frac{\partial \dot{u}}{\partial r} + t_3 \frac{\partial \ddot{u}}{\partial r} \right) - T_0 \beta_{22} \left(\frac{\dot{u}}{r} + t_3 \frac{\ddot{u}}{r} \right) = 0 \tag{16}$$

$$\left(c_{11} + \mu_0 H_0^2 \right) \left(\frac{\partial^2 u}{\partial r^2} + \frac{1}{r} \frac{\partial u}{\partial r} - \frac{c_{22}}{c_{11}} \frac{u}{r^2} \right) - \beta_{11} \left(\frac{\partial \theta}{\partial r} + t_1 \frac{\partial \dot{\theta}}{\partial r} \right) - \frac{1}{r} (\beta_{11} - \beta_{22})(\theta + t_1 \dot{\theta}) = \left(\rho + \varepsilon_0 \mu_0^2 H_0^2 \right) \ddot{u} \tag{17}$$

By considering the same materials properties in 1 and 2 directions, as is seen in Eqs. (16) and (17), these equations reduce to the equations of magneto–thermoelasticity for an isotropic hollow cylinder [46].

To define the boundary conditions for the problem, the heat flux and temperature itself were considered for the inner and the outer boundaries of the cylinder in the form of time-dependent functions:

$$-k \frac{\partial \theta}{\partial r} \Big|_{r=a} = f(t) \tag{18}$$

$$\theta(b,t) = g(t) \tag{19}$$

Also, the thermal initial conditions of the orthotropic cylinder are:

$$\theta(r,0) = F_1(r) \tag{20}$$

$$\dot{\theta}(r,0) = F_2(r) \tag{21}$$

where $F_1(r)$ and $F_2(r)$ are arbitrary functions of the radial position and the superscript dot denotes the partial derivative of the variable with respect to time. For the mechanical boundary conditions, the displacement and traction are applied on the inner and the outer surfaces of the cylinder, respectively:

$$u(a,t) = P_1(t) \tag{22}$$

$$\sigma_{rr}(b,t) = P_2(t) \tag{23}$$

where $P_1(t)$ and $P_2(t)$ are arbitrary time-dependent functions. By substituting Eq. (11) in (23), we will have:

$$\frac{\partial u}{\partial r} \Big|_{r=b} + h_2 u(b,t) = B_2(t) \tag{24}$$

where:

$$h_2 = \frac{c_{12}}{c_{11} b} \tag{25}$$

$$B_2(t) = \frac{1}{c_{11}} P_2(t) + \frac{\beta_{11}}{c_{11}} g(t) \tag{26}$$

The mechanical initial conditions for the problem can be expressed as general functions of the radial position, as follows:

$$u(r,0) = F_3(r) \tag{27}$$

$$\dot{u}(r,0) = F_4(r) \tag{28}$$

3 The method of solution

To simplify the equations, the following parameters were considered to convert the problem into nondimensional form [46]:

$$\hat{r} = c_0 \eta r, \quad \hat{t} = c_0^2 \eta t, \quad \hat{t}_1 = c_0^2 \eta t_1, \quad \hat{t}_2 = c_0^2 \eta t_2, \quad \hat{t}_3 = c_0^2 \eta t_3$$

$$\hat{\sigma}_{rr} = \frac{\sigma_{rr}}{c_{11}}, \quad \hat{\sigma}_{\theta\theta} = \frac{\sigma_{\theta\theta}}{c_{11}}, \quad \hat{\theta} = \theta\alpha_r, \quad \hat{u} = c_0 \eta u, \quad \hat{q}_i = \frac{q_i \alpha_r}{k c_0 \eta}$$

$$\hat{E} = \frac{E_0}{\mu_0 H_0 c_0}, \quad \hat{h} = \frac{1}{H_0} h_0 \tag{29}$$

where:

$$\eta = \frac{\rho c}{k}, c_0 = \sqrt{\frac{c_{11}}{\rho}} \tag{30}$$

c_0 is the velocity of the elastic wave propagation in the medium in the absence of the magnetic field. By applying the nondimensional parameters to Eqs. (14) to (17), and omitting the hat sign for convenience, the nondimensional equations of unified generalized magneto–thermoelasticity in the orthotropic cylinder become:

$$E_0 = \frac{\partial u}{\partial t} \tag{31}$$

$$h_0 = -\left(\frac{u}{r} + \frac{\partial u}{\partial r}\right) \tag{32}$$

$$\frac{\partial^2 \theta}{\partial r^2} + \frac{1}{r}\frac{\partial \theta}{\partial r} - \frac{\partial \theta}{\partial t} - t_2 \frac{\partial^2 \theta}{\partial t^2} - C_1\left(\frac{\partial \dot{u}}{\partial r} + t_3 \frac{\partial \ddot{u}}{\partial r}\right) - C_1 D\left(\frac{\dot{u}}{r} + t_3 \frac{\ddot{u}}{r}\right) = 0 \tag{33}$$

$$\beta_A\left(\frac{\partial^2 u}{\partial r^2} + \frac{1}{r}\frac{\partial u}{\partial r} - \frac{v^2}{r^2}u\right) - C_2\left(\frac{\partial \theta}{\partial r} + t_1 \frac{\partial \dot{\theta}}{\partial r}\right) - \frac{(1-D)}{r}C_2\left(\theta + t_1 \dot{\theta}\right) = \alpha_A \frac{\partial^2 u}{\partial t^2} \tag{34}$$

where:

$$v^2 = \frac{c_{22}}{c_{11}}, \quad C_1 = \frac{T_0 \beta_{11}\alpha_r}{\eta k}, \quad C_2 = \frac{\beta_{11}}{\alpha_r c_{11}}, \quad D = \frac{\beta_{22}}{\beta_{11}}$$

$$\beta_A = 1 + \frac{\mu_0 H_0^2}{c_{11}}, \quad \alpha_A = 1 + \frac{\varepsilon_0 \mu_0^2 H_0^2}{\rho} \tag{35}$$

Coefficient C_1 is the thermomechanical coupling coefficient, and D shows the effect of considering the orthotropic material properties for the cylinder. It can be seen that by considering the same values for the material properties in all directions, coefficients D and v^2 equal 1, which reduces the orthotropic cylinder equations to those for an isotropic cylinder. Also, given the parameters from Eq. (29), the thermal boundary and initial conditions, i.e. Equations (18) to (21), appear as follows:

$$\frac{\partial \theta}{\partial r}\Big|_{r=a} = -\frac{f(t)\alpha_r}{k c_0 \eta} \tag{36}$$

$$\theta(b, t) = g(t)\alpha_r \tag{37}$$

$$\theta(r, 0) = F_1(r)\alpha_r \tag{38}$$

$$\dot{\theta}(r, 0) = \frac{F_2(r)\alpha_r}{c_0^2 \eta} \tag{39}$$

And for the mechanical boundary and initial conditions, we have:

$$u(a, t) = c_0 \eta P_1(t) \tag{40}$$

$$\frac{\partial u}{\partial r}\Big|_{r=b} + h_2 u(b, t) = B_2(t) \tag{41}$$

$$u(r, 0) = c_0 \eta F_3(r) \tag{42}$$

$$\dot{u}(r,0) = \frac{F_4(r)}{c_0} \tag{43}$$

As is seen, Eqs. (33) and (34) are coupled and should be solved simultaneously. By employing the method developed by Shahani and Momeni [47], Eqs. (33) and (34) can be separated into two homogeneous and nonhomogeneous boundary value problems. The boundary conditions are considered to solve the homogeneous equations, and the nonhomogeneous equations, which contain thermo–mechanical coupling terms, should be solved by considering the initial conditions of the problem. The final solutions for the temperature and the displacement fields are the summation of the homogeneous and nonhomogeneous solutions. Accordingly, to solve the unified generalized magneto–thermoelasticity equations, $\theta(r, t)$ and $u(r, t)$ are resolved into two components:

$$u(r,t) = u_1(r,t) + u_2(r,t) \tag{44}$$

$$\theta(r,t) = \theta_1(r,t) + \theta_2(r,t) \tag{45}$$

By applying Eq. (45), the boundary value problem related to Eqs. (18)–(21) are separated into the following two boundary value problems:

$$\frac{\partial^2 \theta_1}{\partial r^2} + \frac{1}{r}\frac{\partial \theta_1}{\partial r} - \frac{\partial \theta_1}{\partial t} - t_2 \frac{\partial^2 \theta_1}{\partial t^2} = 0 \tag{46}$$

$$\frac{\partial \theta_1}{\partial r}\Big|_{r=a} = -\frac{f(t)\alpha_r}{kc_0\eta} \tag{47}$$

$$\theta_1(b,t) = g(t)\alpha_r \tag{48}$$

$$\theta_1(r,0) = 0 \tag{49}$$

$$\dot{\theta}_1(r,0) = 0 \tag{50}$$

and

$$\frac{\partial^2 \theta_2}{\partial r^2} + \frac{1}{r}\frac{\partial \theta_2}{\partial r} - \frac{\partial \theta_2}{\partial t} - t_2 \frac{\partial^2 \theta_2}{\partial t^2} - C_1\left(\frac{\partial \dot{u}}{\partial r} + t_3\frac{\partial \ddot{u}}{\partial r}\right) - C_1 D\left(\frac{\dot{u}}{r} + t_3\frac{\ddot{u}}{r}\right) = 0 \tag{51}$$

$$\frac{\partial \theta_2}{\partial r}\Big|_{r=a} = 0 \tag{52}$$

$$\theta_2(b,t) = 0 \tag{53}$$

$$\theta_2(r,0) = F_1(r)\alpha_r \tag{54}$$

$$\dot{\theta}_2(r,0) = \frac{F_2(r)\alpha_r}{c_0^2\eta} \tag{55}$$

In the same way, Eq. (34) can be resolved into the following boundary value problems by applying the Eq. (44):

$$\beta_A\left(\frac{\partial^2 u_1}{\partial r^2} + \frac{1}{r}\frac{\partial u_1}{\partial r} - \frac{v^2}{r^2}u_1\right) - \alpha_A\ddot{u}_1 = 0 \tag{56}$$

$$u_1(a,t) = c_0\eta P_1(t) \tag{57}$$

$$\frac{\partial u_1}{\partial r}\Big|_{r=b} + h_2 u_1(b,t) = B_2(t) \tag{58}$$

$$u_1(r,0) = 0 \tag{59}$$

$$\dot{u}_1(r,0) = 0 \tag{60}$$

and

$$\beta_A\left(\frac{\partial^2 u_2}{\partial r^2} + \frac{1}{r}\frac{\partial u_2}{\partial r} - \frac{v^2}{r^2}u_2\right) - \alpha_A\ddot{u}_2 = C_2\left(\frac{\partial \theta}{\partial r} + t_1\frac{\partial \dot{\theta}}{\partial r}\right) + \frac{(1-D)}{r}C_2\left(\theta + t_1\dot{\theta}\right) \tag{61}$$

$$u_2(a, t) = 0 \tag{62}$$

$$\frac{\partial u_2}{\partial r}|_{r=b} + h_2 u_2(b, t) = 0 \tag{63}$$

$$u_2(r, 0) = c_0 \eta F_3(r) \tag{64}$$

$$\dot{u}_2(r, 0) = \frac{F_4(r)}{c_0} \tag{65}$$

The Eqs. (46) to (50) and (56) to (60) and can be solved using the finite Hankel transform [48]:

$$H[\theta_1(r, t); \zeta_n] = \overline{\theta}_1(\zeta_n, t) = \int_a^b r\theta_1(r, t) K_1(\zeta_n, r) dr \tag{66}$$

$$H[u_1(r, t); \xi_m] = \overline{u}_1(\xi_m, t) = \int_a^b r u_1(r, t) K_2(\xi_m, r) dr \tag{67}$$

where $K_1(\zeta_n, r)$ and $K_2(\xi_m, r)$ are the kernels of the transformation. The appropriate kernels for the transformation depend on the general form of the equations and the considered boundary conditions for the problem. For the present problem, the kernels of the transformations are defined as follows [48, 49]:

$$K_1(r, \zeta_n) = \mathrm{J}_0(\zeta_n r)\mathrm{Y}_0(\zeta_n b) - \mathrm{J}_0(\zeta_n b)\mathrm{Y}_0(\zeta_n r) \tag{68}$$

$$K_2(r, \xi_m) = \mathrm{J}_\nu(\xi_m r)\mathrm{Y}_\nu(\xi_m a) - \mathrm{J}_\nu(\xi_m a)\mathrm{Y}_\nu(\xi_m r) \tag{69}$$

where ζ_n and ξ_m are the positive roots of the following characteristics equations:

$$\mathrm{J}_0(\zeta_n b)\mathrm{Y}_0'(\zeta_n a) - \mathrm{J}_0'(\zeta_n a)\mathrm{Y}_0(\zeta_n b) = 0 \tag{70}$$

$$\mathrm{Y}_\nu(\xi_m a)\big[\xi_m \mathrm{J}_\nu'(\xi_m b) + h_2 \mathrm{J}_\nu(\xi_m b)\big] - \mathrm{J}_\nu(\xi_m a)\big[\xi_m \mathrm{Y}_\nu'(\xi_m b) + h_2 \mathrm{Y}_\nu(\xi_m b)\big] = 0 \tag{71}$$

The inverses of transformations are defined in the following equations:

$$H^{-1}\big[\overline{\theta}_1(\zeta_n, t); r\big] = \theta_1(r, t) = \sum_{n=1}^{\infty} a_n \overline{\theta}_1(\zeta_n, t) K_1(r, \zeta_n) \tag{72}$$

$$H^{-1}[\overline{u}_1(\xi_m, t); r] = u_1(r, t) = \sum_{m=1}^{\infty} b_m \overline{u}_1(\xi_m, t) K_2(r, \xi_m) \tag{73}$$

where:

$$a_n = \frac{1}{\int_a^b r K_1^2(r, \zeta_n) dr} = \frac{\pi^2}{2} \frac{\zeta_n^2 \{\mathrm{J}_0'(\zeta_n a)\}^2}{\{\mathrm{J}_0'(\zeta_n a)\}^2 - \{\mathrm{J}_0(\zeta_n b)\}^2} \tag{74}$$

$$b_m = \frac{1}{\int_a^b r K_2^2(r, \xi_m) dr} = \frac{\pi^2 \xi_m^2 e_2^2}{2\{(\mathrm{J}_\nu(\xi_m a))^2\}(h_2^2 + \xi_m^2[1 - (\frac{\nu}{\xi_m b})^2]) - e_2^2} \tag{75}$$

in which

$$e_2 = \xi_m \mathrm{J}_\nu'(\xi_m b) + h_2 \mathrm{J}_\nu(\xi_m b) \tag{76}$$

Applying the finite Hankel transform to the Eqs. (46) and (56), results in:

$$t_2 \frac{\partial^2 \overline{\theta}_1}{\partial t^2} + \frac{\partial \overline{\theta}_1}{\partial t} + \zeta_n^2 \overline{\theta}_1(\zeta_n, t) = \left[\frac{2}{\pi} g(t) - \frac{2\mathrm{J}_0(\zeta_n b)}{\pi \zeta_n \mathrm{J}_0'(\zeta_n a)} f(t)\right] = A_1(t) \tag{77}$$

$$\frac{\partial^2 \overline{u}_1(\xi_m, t)}{\partial t^2} + \left(\frac{\xi_m}{\gamma}\right)^2 \overline{u}_1(\xi_m, t) = \frac{1}{\gamma^2}\left[\frac{2\mathrm{J}_\nu(\xi_m a)}{\pi e_2} B_2(t) - \frac{2}{\pi} B_1(t)\right] = A_2(t) \tag{78}$$

By comparing Eqs. (56) and (78), it can be seen that both sides were divided by α_A, and for the new parameter γ, we have:

$$\gamma = \sqrt{\frac{\alpha_A}{\beta_A}} \tag{79}$$

Solutions for Eqs. (77) and (78), which are non-homogeneous ordinary differential equations, can be obtained in the following form:

$$\bar{\theta}_1(\zeta_n, t) = \frac{2}{\Delta} \int_0^t A_1(\tau) e^{\frac{-1}{2t_2}(t-\tau)} \sin\left(\frac{\Delta}{2t_2}(t-\tau)\right) d\tau \tag{80}$$

$$\bar{u}_1(\xi_m, t) = \frac{\gamma}{\xi_m} \int_0^t A_2(\tau) \sin\left(\frac{\gamma}{\xi_m}(t-\tau)\right) d\tau \tag{81}$$

where $\Delta = \sqrt{4t_2\zeta_n^2 - 1}$. Using the inversion relations of the transformation for Eqs. (72) and (73), we have:

$$\theta_1(r, t) = \sum_{n=1}^{\infty} a_n K_1(r, \zeta_n) \frac{2}{\Delta} \int_0^t A_1(\tau) e^{\frac{-1}{2t_2}(t-\tau)} \sin\left((t-\tau)\frac{\Delta}{2t_2}\right) d\tau \tag{82}$$

$$u_1(r, t) = \sum_{m=1}^{\infty} \frac{\gamma}{\xi_m} b_m K_2(r, \xi_m) \int_0^t A_2(\tau) \sin\left(\frac{\gamma}{\xi_m}(t-\tau)\right) d\tau \tag{83}$$

As is seen, Eqs. (82) and (83) are the solution of the homogeneous parts of the equations. To solve the nonhomogeneous set of the equations the following forms can be considered for $\theta_2(r, t)$ and $u_2(r, t)$ [47]:

$$\theta_2(r, t) = \sum_{n=1}^{\infty} Q(t) K_1(r, \zeta_n) \tag{84}$$

$$u_2(r, t) = \sum_{m=1}^{\infty} S(t) K_2(r, \xi_m) \tag{85}$$

where $Q(t)$ and $S(t)$ are functions of time that should be calculated. It is worth noting that, the considered forms for $\theta_2(r, t)$ and $u_2(r, t)$ satisfy the related boundary conditions, hence (52), (53) and (62), (63). Substituting Eqs. (72), (73) and (84) and (85) yields:

$$\left(t_2\ddot{Q} + \dot{Q} + \zeta_n^2 Q\right) K_1(r, \zeta_n) = -C_1\left[b_m\dot{\bar{u}}_1 + \dot{S} + t_3\left(b_m\ddot{\bar{u}}_1 + \ddot{S}\right)\right]\left[\left(\frac{\partial K_2(r, \xi_m)}{\partial r}\right) + D\left(\frac{K_2(r, \xi_m)}{r}\right)\right] \tag{86}$$

$$\left(\gamma^2\ddot{S} + \xi_m^2 S\right) K_2(r, \xi_m) = -\frac{C_2}{\beta_A}\left[a_n\bar{\theta}_1 + Q + t_1\left(a_n\dot{\bar{\theta}}_1 + \dot{Q}\right)\right]\left[\frac{\partial K_1(r, \zeta_n)}{\partial r} + \frac{1}{r}(1-D)K_1(r, \zeta_n)\right] \tag{87}$$

Using the orthogonal property of Bessel functions we have:

$$\int_a^b r K_1(r, \zeta_n) K_1(r, \zeta_p) dr = N_n \delta_{np} \tag{88}$$

$$\int_a^b r K_2(r, \xi_m) K_2(r, \xi_p) dr = M_m \delta_{mp} \tag{89}$$

where δ is the Kronecker delta and:

$$N_n = \frac{\pi^2}{2} \frac{\zeta_n^2 \{J_0'(\zeta_n a)\}^2}{\{J_0'(\zeta_n a)\}^2 - \{J_0(\zeta_n b)\}^2} \tag{90}$$

$$M_m = \frac{\pi^2 \xi_m^2 e_2^2}{2\{(J_\nu(\xi_m a))^2\}(h_2^2 + \xi_m^2[1 - (\frac{\nu}{\xi_m b})^2]) - e_2^2} \tag{91}$$

e_2 is defined in Eq. (76). Multiplying Eqs. (86) and (87) by $r K_1(r, \zeta_n)$ and $r K_2(r, \xi_m)$ respectively, integrating between a and b, and then using the orthogonality relations, leads to:

$$t_2 \dddot{Q} + \dot{Q} + \zeta_n^2 Q = \left\{ -\frac{C_1 \int_a^b r K_1(r, \zeta_n) \left[\left(\frac{\partial K_2(r, \xi_m)}{\partial r} \right) + D \left(\frac{K_2(r, \xi_m)}{r} \right) \right] dr}{N_n} \right\} \left(b_m \dot{\bar{u}}_1 + \dot{S} + t_3 (b_m \ddot{\bar{u}}_1 + \ddot{S}) \right) \quad (92)$$

$$\ddot{S} + \left(\frac{\xi_m}{\gamma} \right)^2 S = \frac{C_2}{\beta_A} \left\{ -\frac{\int_a^b r K_2(r, \xi_m) \left[\frac{\partial K_1(r, \zeta_n)}{\partial r} + \frac{1}{r} (1 - D) K_1(r, \zeta_n) \right] dr}{M_m} \right\} \left[a_n \bar{\theta}_1 + Q + t_1 \left(a_n \dot{\bar{\theta}}_1 + \dot{Q} \right) \right]$$
$$(93)$$

The following parameters are defined for convenience:

$$U_1 = \left\{ -\frac{\int_a^b r K_1(r, \zeta_n) \left[\left(\frac{\partial K_2(r, \xi_m)}{\partial r} \right) + D \left(\frac{K_2(r, \xi_m)}{r} \right) \right] dr}{N_n} \right\} \quad (94)$$

$$U_2 = \frac{C_2}{\gamma^2 \beta_A} \left\{ -\frac{\int_a^b r K_2(r, \xi_m) \left[\frac{\partial K_1(r, \zeta_n)}{\partial r} + \frac{1}{r} (1 - D) K_1(r, \zeta_n) \right] dr}{M_m} \right\} \quad (95)$$

Now, Eqs. (92) and (93) can be written in the following forms:

$$t_2 \dddot{Q} + \dot{Q} + \zeta_n^2 Q = C_1 U_1 \left((b_m \dot{\bar{u}}_1 + \dot{S}) + t_3 (b_m \ddot{\bar{u}}_1 + \ddot{S}) \right) \quad (96)$$

$$\ddot{S} + \left(\frac{\xi_m}{\gamma} \right)^2 S = U_2 \left((a_n \bar{\theta}_1 + Q) + t_1 \left(a_n \dot{\bar{\theta}}_1 + \dot{Q} \right) \right) \quad (97)$$

By substituting Eq. (54) and (55) into (84), the appropriate form for the initial conditions of the problem can be obtained as:

$$Q(0) K_1(r, \zeta_n) = F_1(r) \quad (98)$$

$$\dot{Q}(0) K_1(r, \zeta_n) = F_2(r) \quad (99)$$

Applying the orthogonality relation, Eq. (88), to Eqs. (98) and (99) leads to:

$$Q(0) = \frac{\int_a^b r K_1(r, \zeta_n) F_1(r) dr}{N_n} \quad (100)$$

$$\dot{Q}(0) = \frac{\int_a^b r K_1(r, \zeta_n) F_2(r) dr}{N_n} \quad (101)$$

The initial conditions for the nonhomogeneous part of the displacement equation, i.e. $S(t)$, can be obtained in the same manner:

$$S(0) = \frac{\int_a^b r K_2(r, \xi_m) F_3(r) dr}{M_m} \quad (102)$$

$$\dot{S}(0) = \frac{\int_a^b r K_2(r, \xi_m) F_4(r) dr}{M_m} \quad (103)$$

It can be seen that Eqs. (96) and (97) are coupled, but they can be uncoupled by performing some mathematical operations [38]. Differentiating Eqs. (96) and (97) with respect to time leads to:

$$t_2 \ddddot{Q} + \dddot{Q} + \zeta_n^2 \dot{Q} = C_1 U_1 \left((b_m \ddot{\bar{u}}_1 + \ddot{S}) + t_3 (b_m \dddot{\bar{u}}_1 + \dddot{S}) \right) \quad (104)$$

$$\dddot{S} + \left(\frac{\xi_m}{\gamma} \right)^2 \dot{S} = U_2 \left((a_n \dot{\bar{\theta}}_1 + \dot{Q}) + t_1 \left(a_n \ddot{\bar{\theta}}_1 + \ddot{Q} \right) \right) \quad (105)$$

$$t_2 Q^{(4)} + \dddot{Q} + \zeta_n^2 \ddot{Q} = C_1 U_1 \left(\left(b_m \dddot{\bar{u}}_1 + \dddot{S} \right) + t_3 \left(b_m \bar{u}_1^{(4)} + S^{(4)} \right) \right) \quad (106)$$

$$S^{(4)} + \left(\frac{\xi_m}{\gamma}\right)^2 \ddot{S} = U_2\left(\left(a_n\ddot{\bar{\theta}}_1 + \ddot{Q}\right) + t_1\left(a_n\dddot{\bar{\theta}}_1 + \dddot{Q}\right)\right) \tag{107}$$

Substituting $\dddot{Q}$ and $\dddot{Q}$ from Eqs. (96) and (97) in the Eq. (107) results in:

$$S^{(4)} + \left(\frac{\xi_m}{\gamma}\right)^2 \ddot{S} = U_2\left\{a_n\ddot{\bar{\theta}}_1 + \frac{1}{t_2}C_1U_1\left[(b_m\dot{\bar{u}}_1 + \dot{S}) + t_3(b_m\ddot{\bar{u}}_1 + \ddot{S})\right] - \frac{1}{t_2}\dot{Q} - \frac{1}{t_2}\zeta_n^2 Q\right.$$
$$\left. + t_1\left(a_n\dddot{\bar{\theta}}_1 + \frac{1}{t_2}C_1U_1\left[(b_m\ddot{\bar{u}}_1 + \ddot{S}) + t_3(b_m\dddot{\bar{u}}_1 + \dddot{S})\right] - \frac{1}{t_2}\ddot{Q} - \frac{1}{t_2}\zeta_n^2\dot{Q}\right)\right\} \tag{108}$$

By ordering the above equation and separating Q and $\dot{Q}$ terms we will have:

$$S^{(4)} + \left(\frac{\xi_m}{\gamma}\right)^2 \ddot{S} = U_2\left\{a_n\ddot{\bar{\theta}}_1 + \frac{1}{t_2}C_1U_1\left[(b_m\dot{\bar{u}}_1 + \dot{S}) + t_3(b_m\ddot{\bar{u}}_1 + \ddot{S})\right]\right.$$
$$\left. + t_1\left(a_n\dddot{\bar{\theta}}_1 + \frac{1}{t_2}C_1U_1\left[(b_m\ddot{\bar{u}}_1 + \ddot{S}) + t_3(b_m\dddot{\bar{u}}_1 + \dddot{S})\right]\right) - \frac{1}{t_2}(\dot{Q} + t_1\ddot{Q}) - \frac{\zeta_n^2}{t_2}(Q + t_1\dot{Q})\right\} \tag{109}$$

Now, by substituting $Q + t_1\dot{Q}$ and $\dot{Q} + t_1\ddot{Q}$ from Eqs. (97), and (105), into Eq. (109) we have:

$$t_2 S^{(4)} + [1 - C_1U_1U_2t_1t_3]\dddot{S} + \left[t_2\left(\frac{\xi_m}{\gamma}\right)^2 + \zeta_n^2 - C_1t_3U_1U_2 - C_1t_1U_1U_2\right]\ddot{S}$$
$$+ \left[\left(\frac{\xi_m}{\gamma}\right)^2 - C_1U_1U_2\right]\dot{S} + \left(\frac{\xi_m}{\gamma}\right)^2\zeta_n^2 S$$
$$= U_2\left[a_n\left(t_2\ddot{\bar{\theta}}_1 + \dot{\bar{\theta}}_1 + \zeta_n^2\bar{\theta}_1\right) + a_nt_1\left(t_2\dddot{\bar{\theta}}_1 + \ddot{\bar{\theta}}_1 + \zeta_n^2\dot{\bar{\theta}}_1\right) + C_1U_1b_m\left(\dot{\bar{u}}_1 + t_3\ddot{\bar{u}}_1\right) + t_1C_1U_1b_m\left(\ddot{\bar{u}}_1 + t_3\dddot{\bar{u}}_1\right)\right] \tag{110}$$

As is seen, the above equation is independent of Q and can be solved individually. Substituting $S^{(4)}$ from Eq. (107) into Eq. (106) yields:

$$t_2 Q^{(4)} + \dddot{Q} + \zeta_n^2\ddot{Q} = C_1U_1\left\{b_m\dddot{\bar{u}}_1 + U_2\left[\left(a_n\dot{\bar{\theta}}_1 + \dot{Q}\right) + t_1\left(a_n\ddot{\bar{\theta}}_1 + \ddot{Q}\right)\right]\right.$$
$$\left. + t_3\left(b_m\bar{u}_1^{(4)} + U_2\left[\left(a_n\ddot{\bar{\theta}}_1 + \ddot{Q}\right) + t_1\left(a_n\dddot{\bar{\theta}}_1 + \dddot{Q}\right)\right]\right) - \left(\frac{\xi_m}{\gamma}\right)^2(\dot{S} + t_3\ddot{S})\right\} \tag{111}$$

Now, by substituting $\dot{S} + t_3\ddot{S}$ from Eq. (96) into Eq. (111) we have:

$$t_2 Q^{(4)} + [1 - C_1U_1U_2t_1t_3]\dddot{Q} + \left[t_2\left(\frac{\xi_m}{\gamma}\right)^2 + \zeta_n^2 - C_1t_3U_1U_2 - C_1t_1U_1U_2\right]\ddot{Q}$$
$$+ \left[\left(\frac{\xi_m}{\gamma}\right)^2 - C_1U_1U_2\right]\dot{Q} + \left(\frac{\xi_m}{\gamma}\right)^2\zeta_n^2 Q$$
$$= C_1U_1\left\{b_m\left(\dddot{\bar{u}}_1 + \left(\frac{\xi_m}{\gamma}\right)^2\dot{\bar{u}}_1\right) + t_3b_m\left(\bar{u}_1^{(4)} + \left(\frac{\xi_m}{\gamma}\right)^2\ddot{\bar{u}}_1\right) + U_2a_n\left[\left(\dot{\bar{\theta}}_1 + t_1\ddot{\bar{\theta}}_1\right) + t_3\left(\ddot{\bar{\theta}}_1 + t_1\dddot{\bar{\theta}}_1\right)\right]\right\} \tag{112}$$

Substituting $A_1(t)$ and $A_2(t)$ from Eqs. (77) and (78) into Eqs. (110) and (112) results in:

$$t_2\frac{d^4 S}{dt^4} + [1 - C_1U_1U_2t_1t_3]\frac{d^3 S}{dt^3} + \left[t_2\left(\frac{\xi_m}{\gamma}\right)^2 + \zeta_n^2 - C_1t_3U_1U_2 - C_1t_1U_1U_2\right]\frac{d^2 S}{dt^2}$$

$$+ \left[\left(\frac{\xi_m}{\gamma} \right)^2 - C_1 U_1 U_2 \right] \frac{dS}{dt} + \left(\frac{\xi_m}{\gamma} \right)^2 \zeta_n^2 S$$

$$= U_2 \left\{ a_n \left[A_1(t) + t_1 \dot{A}_1(t) \right] + C_1 U_1 b_m \left[\left(\dot{\bar{u}}_1 + t_1 \ddot{\bar{u}}_1 \right) + t_3 \left(\ddot{\bar{u}}_1 + t_1 \dddot{\bar{u}}_1 \right) \right] \right\} \tag{113}$$

$$t_2 \frac{d^4 Q}{dt^4} + [1 - C_1 U_1 U_2 t_1 t_3] \frac{d^3 Q}{dt^3} + \left[t_2 \left(\frac{\xi_m}{\gamma} \right)^2 + \zeta_n^2 - C_1 t_3 U_1 U_2 - C_1 t_1 U_1 U_2 \right] \frac{d^2 Q}{dt^2}$$

$$+ \left[\left(\frac{\xi_m}{\gamma} \right)^2 - C_1 U_1 U_2 \right] \frac{dQ}{dt} + \left(\frac{\xi_m}{\gamma} \right)^2 \zeta_n^2 Q$$

$$= C_1 U_1 \left\{ b_m \left(\dot{A}_2(t) + t_3 \ddot{A}_2(t) \right) + U_2 a_n \left[\left(\dot{\bar{\theta}}_1 + t_1 \ddot{\bar{\theta}}_1 \right) + t_3 \left(\ddot{\bar{\theta}}_1 + t_1 \dddot{\bar{\theta}}_1 \right) \right] \right\} \tag{114}$$

As is seen, Eqs. (113) and (114) are ordinary differential equations, and $Q(t, \zeta_n)$ and $S(t, \xi_m)$ can be obtained by solving these equations. The solutions of the Eqs. (113) and (114), depend on the initial conditions of the problem; therefore, final solutions for $Q(t)$ and $S(t)$ are presented in the numerical example and discussion section. Now, the solutions for both parts of $\theta(r, t)$ and $u(r, t)$ are obtained and the closed-form relations for temperature and displacement are summation of these parts:

$$\theta(r,t) = \sum_{n=1}^{\infty} a_n \bar{\theta}_1(t) K_1(r, \zeta_n) + \sum_{m=1}^{\infty} \sum_{n=1}^{\infty} Q(t) K_1(r, \zeta_n) \tag{115}$$

$$u(r,t) = \sum_{m=1}^{\infty} b_m \bar{u}_1(t) K_2(r, \xi_m) + \sum_{m=1}^{\infty} \sum_{n=1}^{\infty} S(t) K_2(r, \xi_m) \tag{116}$$

It is important to note that the presented method in this work can be employed to address a wide range of problems associated with different types of boundary conditions, including Cauchy, Neumann and Dirichlet, for both the heat conduction equation and the equation of motion.

4 Numerical example and discussion

To investigate the magneto–thermoelastic response of the orthotropic cylinder subjected to a thermal shock and a magnetic field, the following material properties are considered:

$$a = 1 \text{ m}, \quad b = 2 \text{ m}, \quad T_0 = 298.15$$

$$k = 0.5 \text{ W/mK}, \quad \rho = 2707 \text{ kg/m}^3, \quad c = 263 \frac{J}{\text{kg K}}$$

$$E_{11} = 19.8 \text{ GPa}, \quad E_{22} = 48.3 \text{ GPa}, \quad E_{33} = 19.8 \text{ GPa}, \quad G_{12} = 8.9 \text{ GPa}$$

$$G_{23} = 8.9 \text{ GPa}, \quad G_{31} = 6.19 \text{ GPa}, \quad v_{12} = 0.27, \quad v_{23} = 0.27, \quad v_{31} = 0.3$$

$$\alpha_{11} = 15 \times 10^{-6} \text{ 1/K}, \quad \alpha_{22} = 23 \times 10^{-6} \text{ 1/K}, \quad \alpha_{33} = 15 \times 10^{-6} \text{ 1/K}$$

$$\varepsilon_0 = 8.854 \times 10^{-12} \text{ F/m}, \quad \mu_0 = 4\pi \times 10^{-7} \text{ H/m}$$

The inner boundary of the orthotropic cylinder is constrained and subjected to a constant heat flux, while the outer boundary is traction-free with its temperature remaining constant. The thermal and the mechanical boundary conditions for this problem are:

$$-\frac{\partial \theta}{\partial r} \Big|_{r=a} = q_{in} \tag{117}$$

$$\theta(b, t) = 0 \tag{118}$$

$$u(a, t) = 0 \tag{119}$$

$$\sigma_{rr}(b,t) = \frac{\partial u}{\partial r} \Big|_{r=b} + h_2 u(b,t) = 0 \tag{120}$$

Also, the thermal and mechanical initial conditions are:

$$\theta(r,0) = 0 \tag{121}$$

$$\dot{\theta}(r,0) = 0 \tag{122}$$

$$u(r,0) = 0 \tag{123}$$

$$\dot{u}(r,0) = 0 \tag{124}$$

Thus, we have:

$$Q(0) = 0 \tag{125}$$

$$\dot{Q}(0) = 0 \tag{126}$$

$$S(0) = 0 \tag{127}$$

$$\dot{S}(0) = 0 \tag{128}$$

Using the thermal boundary conditions and Eq. (77) leads to:

$$A_1(t) = \frac{2J_0(\zeta_n b)}{\pi \zeta_n J_0'(\zeta_n a)} q_{in} \tag{129}$$

$$\overline{\theta}_1(\zeta_n, t) = \frac{4}{\Delta} \frac{J_0(\zeta_n b)}{\pi \zeta_n J_0'(\zeta_n a)} \int_0^t q_{in}(\tau) e^{\frac{-1}{2t_2}(t-\tau)} \sin\left((t-\tau)\frac{\Delta}{2t_2}\right) d\tau \tag{130}$$

Using the mechanical boundary conditions and Eq. (26) we will have:

$$B_2 = 0 \tag{131}$$

$$A_2(t) = 0 \tag{132}$$

Substituting Eq. (132) into Eq. (81) gives:

$$\overline{u}_1(\xi_m, t) = 0 \tag{133}$$

Substituting Eqs. (130) and (133) into Eqs. (82) and (83) gives:

$$\theta_1(r,t) = \sum_{n=1}^{\infty} a_n \frac{4}{\Delta} \frac{J_0(\zeta_n b)}{\pi \zeta_n J_0'(\zeta_n a)} \frac{2q_{in}}{\Delta(\Delta^2+1)} \left(\Delta t_2 - t_2 \exp\left(-\frac{t}{2t_2}\right)\left[\sin\left(\frac{\Delta t}{2t_2}\right) + \Delta \cos\left(\frac{\Delta t}{2t_2}\right)\right]\right) K_1(r,\zeta_n) \tag{134}$$

$$u_1(r,t) = 0 \tag{135}$$

Therefore, Eqs. (113) and (114) give the following equations:

$$t_2 \frac{d^4 S}{dt^4} + [1 - C_1 U_1 U_2 t_1 t_3] \frac{d^3 S}{dt^3} + \left[t_2\left(\frac{\xi_m}{\gamma}\right)^2 + \zeta_n^2 - C_1 t_3 U_1 U_2 - C t_1 U_1 U_2\right] \frac{d^2 S}{dt^2}$$
$$+ \left[\left(\frac{\xi_m}{\gamma}\right)^2 - C_1 U_1 U_2\right] \frac{dS}{dt} + \left(\frac{\xi_m}{\gamma}\right)^2 \zeta_n^2 S = U_2\left[a_n \frac{2J_0(\zeta_n b)}{\pi \zeta_n J_0'(\zeta_n a)}\right] \tag{136}$$

$$t_2 \frac{d^4 Q}{dt^4} + [1 - C_1 U_1 U_2 t_1 t_3] \frac{d^3 Q}{dt^3} + \left[t_2\left(\frac{\xi_m}{\gamma}\right)^2 + \zeta_n^2 - C_1 t_3 U_1 U_2 - C_1 t_1 U_1 U_2\right] \frac{d^2 Q}{dt^2}$$
$$+ \left[\left(\frac{\xi_m}{\gamma}\right)^2 - C_1 U_1 U_2\right] \frac{dQ}{dt} + \left(\frac{\xi_m}{\gamma}\right)^2 \zeta_n^2 Q = C_1 U_1 \left\{U_2 a_n\left[\left(\dot{\overline{\theta}}_1 + t_1 \ddot{\overline{\theta}}_1\right) + t_3\left(\ddot{\overline{\theta}}_1 + t_1 \dddot{\overline{\theta}}_1\right)\right]\right\} \tag{137}$$

Terms $\dot{\overline{\theta}}_1$, $\ddot{\overline{\theta}}_1$ and $\dddot{\overline{\theta}}_1$ can be calculated by differentiating Eq. (130). The solution of Eq. (136) can be obtained in the following form:

$$S(t) = \frac{2q_{in}U_2a_n\mathrm{J}_0(\zeta_n b)}{\pi\left(\frac{\xi_m}{\gamma}\right)^2\zeta_n^3\mathrm{J}_0'(\zeta_n a)} + \sum_{i=1}^{4} c_i e^{\alpha_i t} \tag{138}$$

$Q(t)$ can be calculated using $S(t)$ and Eqs. (96), (97), (104) and (105) in the following form:

$$Q(t) = Z_1\frac{d^3S}{dt^3} + Z_2\frac{d^2S}{dt^2} + Z_3\frac{dS}{dt} + Z_4 S - \frac{t_2 - t_1}{t_1^2\zeta_n^2 + t_2 - t_1}a_n\overline{\theta}_1 \tag{139}$$

where:

$$Z_1 = -\frac{t_1 t_2}{U_2\left(t_1^2\zeta_n^2 + t_2 - t_1\right)} \tag{140}$$

$$Z_2 = -\frac{-t_1^2 C_1 U_1 U_2 t_3 - t_2 + t_1}{U_2\left(t_1^2\zeta_n^2 + t_2 - t_1\right)} \tag{141}$$

$$Z_3 = -\frac{t_1 t_2\left(\frac{\xi_m}{\gamma}\right)^2 - t_1^2 C_1 U_1 U_2}{U_2\left(t_1^2\zeta_n^2 + t_2 - t_1\right)} \tag{142}$$

$$Z_4 = -\frac{-(t_2 - t_1)\left(\frac{\xi_m}{\gamma}\right)^2}{U_2\left(t_1^2\zeta_n^2 + t_2 - t_1\right)} \tag{143}$$

Substituting Eq. (138) into Eq. (139) leads to:

$$Q(t) = Z_4\frac{2q_{in}U_2a_n\mathrm{J}_0(\zeta_n b)}{\pi\left(\frac{\xi_m}{\gamma}\right)^2\zeta_n^3\mathrm{J}_0'(\zeta_n a)} - \frac{t_2 - t_1}{t_1^2\zeta_n^2 + t_2 - t_1}a_n\overline{\theta}_1 + \sum_{i=1}^{4}(Z_1\alpha_i^3 + Z_2\alpha_i^2 + Z_3\alpha_i + Z_4)c_i e^{\alpha_i t} \tag{144}$$

where α_i's are the roots of following characteristic equation:

$$t_2 x^4 + (1 - C_1 U_1 U_2 t_1 t_3)x^3 + \left(t_2\left(\frac{\xi_m}{\gamma}\right)^2 + \zeta_n^2 - C_1 t_3 U_1 U_2 - C_1 t_1 U_1 U_2\right)x^2$$
$$+ \left(\left(\frac{\xi_m}{\gamma}\right)^2 - C_1 U_1 U_2\right)x + \left(\frac{\xi_m}{\gamma}\right)^2\zeta_n^2 = 0 \tag{145}$$

Also, the c_i can be obtained using Eqs. (125) to (128).

$$\begin{pmatrix} c_1 \\ c_2 \\ c_3 \\ c_4 \end{pmatrix} = \begin{pmatrix} 1 & 1 & 1 & 1 \\ \alpha_1 & \alpha_2 & \alpha_3 & \alpha_4 \\ Y_1 & Y_2 & Y_3 & Y_4 \\ \alpha_1 Y_1 & \alpha_2 Y_2 & \alpha_3 Y_3 & \alpha_4 Y_4 \end{pmatrix}^{-1}\begin{pmatrix} R_1 \\ 0 \\ R_2 \\ 0 \end{pmatrix} \tag{146}$$

where:

$$Y_1 = Z_1\alpha_1^3 + Z_2\alpha_1^2 + Z_3\alpha_1 + Z_4 \tag{147}$$

$$Y_2 = Z_1\alpha_2^3 + Z_2\alpha_2^2 + Z_3\alpha_2 + Z_4 \tag{148}$$

$$Y_3 = Z_1\alpha_3^3 + Z_2\alpha_3^2 + Z_3\alpha_3 + Z_4 \tag{149}$$

$$Y_4 = Z_1\alpha_4^3 + Z_2\alpha_4^2 + Z_3\alpha_4 + Z_4 \tag{150}$$
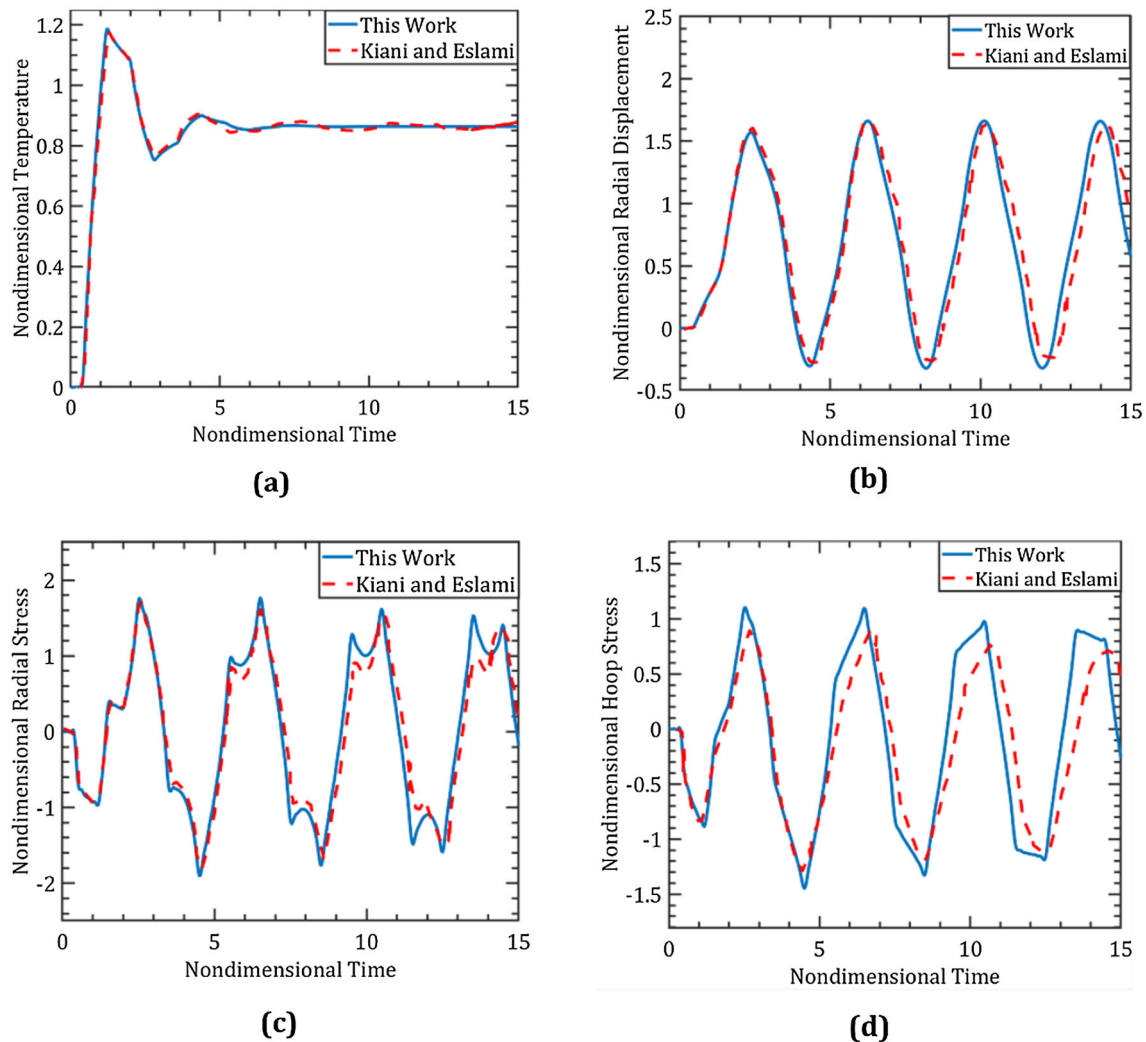
Fig. 2 Comparison between the results of the current study and the GDQ results presented by Kiani and Eslami [34] for the history of nondimensional **a)** temperature **b)** radial displacement **c)** radial stress and **d)** hoop stress at the mid-radius of the isotropic stationary disk based on the Lord–Shulman theory. $t_2 = 0$, $t_2 = t_3 = 0.64$, $q_i = 3$ and $C_1 = 0.0082594$

and:

$$R_1 = -\frac{2q_{in}U_2 a_n \mathrm{J}_0(\zeta_n b)}{\pi \left(\frac{\xi_m}{\gamma}\right)^2 \zeta_n^3 \mathrm{J}_0'(\zeta_n a)}, \quad R_2 = -\frac{(t_2 - t_1)}{(t_1^2 \zeta_n^2 + t_2 - t_1)} \frac{2q_{in} a_n \mathrm{J}_0(\zeta_n b)}{\pi \zeta_n^3 \mathrm{J}_0'(\zeta_n a)} \quad (151)$$

To validate the accuracy of the presented solution in the current work, the special case of an isotropic disk subjected to a thermal shock based on the Lord–Shulman was considered [34]. The isotropic cylinders are specific form of the orthotropic ones where the material properties are same in all directions. Furthermore, the presented solution in this work was developed based on the elastic constants and it can be utilized to study the response of the disks by employing plane stress relations in Eq. (3). Figure 2 presents the history of nondimensional temperature, nondimensional radial displacement, nondimensional radial stress and nondimensional hoop stress in an isotropic disk based on the Lord–Shulman theory at $r = 1.5$. For these plots, $t_2 = 0$, $t_2 = t_3 = 0.64$, $q_i = 3$ and $C_1 = 0.0082594$ were considered. It can be seen that reducing the current problem to the special case of the isotropic material leads to good agreement with the presented results by Kiani and Eslami [34], using the GDQ method.

Figure 3 shows the through-thickness distribution of the nondimensional temperature, nondimensional radial displacement, nondimensional radial and hoop stresses and nondimensional induced magnetic and

electric fields for the orthotropic cylinder based on the Lord–Shulman theory at $t = 0.5$. As seen in Fig. 3a, applying a magnetic field with higher intensity does not change the distribution of the temperature. Although applying the magnetic field does not change the velocity of the temperature wave, considering Eqs. (16) and (17), it is evident that the effect of applying magnetic fields appears in the displacement equation. This change in the displacement field reflects in the heat conduction equation through the coupling term, C_1. Since the coupling term for the orthotropic cylinder is smaller than the isotropic one ($C_{isotropic} = 0.0082$ compared to $C_{orthotropic} = 0.0036$), the effect of applying the magnetic field cannot be detected in the figures related to the temperature distribution.

As it is depicted in Fig. 3b, increasing the intensity of the magnetic field reduces the magnitude of the displacement. The velocity of the displacement wave can be calculated using the following formula:

$$V_e = \sqrt{\frac{\beta_A}{\alpha_A}} = \sqrt{\frac{1 + \frac{\mu_0 H_0^2}{c_{11}}}{1 + \frac{\varepsilon_0 \mu_0^2 H_0^2}{\rho}}} \qquad (152)$$

As is seen, while for the $H_0 = \frac{1}{4\pi} * 10^7$ the velocity of the propagated elastic wave equals 1.000014, for the case of $H_0 = \frac{1}{4\pi} * 10^9$ it increases to 1.133792. This indicates that the elastic wave reaches radial positions at earlier times for higher intensities of the applied magnetic field. This phenomenon can be observed in Fig. 3c, d where nondimensional radial and hoop stresses were plotted at $t = 0.5$. At this moment, the peak values for the lower intensity of the magnetic field are behind those related to the higher intensity. As indicated by Eqs. (33) and (34), induced magnetic and electrical fields are functions of the displacement, therefore and as illustrated in Fig. 2e, f, both variables decrease for the higher value of the applied magnetic field.

Figure 4 depicts the history of nondimensional temperature, radial displacement, radial stress and hoop stress for different radial positions. As is seen in Fig. 4a, a sudden change happens in the temperature at initial moments of applying thermal shock which is a consequence of considering finite speed for the temperature wave. The velocity of the propagated temperature wave can be obtained using the following equation:

$$V_t = \sqrt{\frac{1}{t_2}} = 1.00 \qquad (153)$$

The effects of the boundary conditions on the propagation and the reflection of the stress wave can be seen in Fig. 4c, d. The generated dilatation wave at the inner surface of the cylinder propagates forward into the medium and upon reaching the outer surface, it reflects back into the medium in the opposite direction, adhering to the traction-free boundary condition (Cauchy boundary condition) imposed on the outer surface of the cylinder. Conversely, displacement-type boundary condition (Dirichlet boundary condition), on the inner boundary leads to the reflection in the same direction. It is important to note that, due to lumped assumption in the flexural components such as beams, plates and shells, the temperature and stress wave fronts do not appear in these components by applying thermal shocks [3].

Figure 5 illustrates the through-thickness distributions of nondimensional temperature, displacement, radial and hoop stresses and magnetic and electric fields for different times based on the Lord–Shulman theory. As it can be seen in Fig. 5a, at $r = 1$, temperature wave initiates at about 0.4 and goes to zero at mid radius of the cylinder which indicates that wave front is at $r = 1.5$ at Time $= 0.5$. Additionally, at Time $= 1$, the temperature wave front reaches $r = 2$, which is consistent with the considered velocity ($t_2 = t_3 = 1$) for the temperature wave. Figure 5b shows that the constrained boundary condition on the inner surface of the cylinder leads to outward expansion. As it was indicated in Eq. (120), the outer surface of the cylinder is traction-free, and this can be seen in Fig. 5c, where the radial stress is zero at $r = 2$ for different times.

The elastic wave fronts for the radial and hoop stresses can be observed in Fig. 5c, d. For example, at Time $= 0.5$, the elastic wave is at $r = 1.5$, and before this moment, both stress components are zero. Similarly, at Time $= 1.5$, the reflected wave from the outer boundary can be observed re-entering the cylinder, but with a reversed sign. Similarly, as depicted in Fig. 5e, f, induced magnetic and electric waves reach all radial positions concurrently with the elastic wave.

Figure 6 illustrates the history of nondimensional temperature, radial displacement, radial and hoop stresses based on the Green–Lindsay theory. As is seen in Fig. 6a, as time passes, steep jump in the temperature disappears, and the temperature becomes steady at the mid-radius of the cylinder after Time $= 4$, which is the result of the increasing the temperature of the medium. In addition, the steep jump in the stress components histories at the initial moments of applying thermal shock is clearly shown in these figures. Considering Eqs.
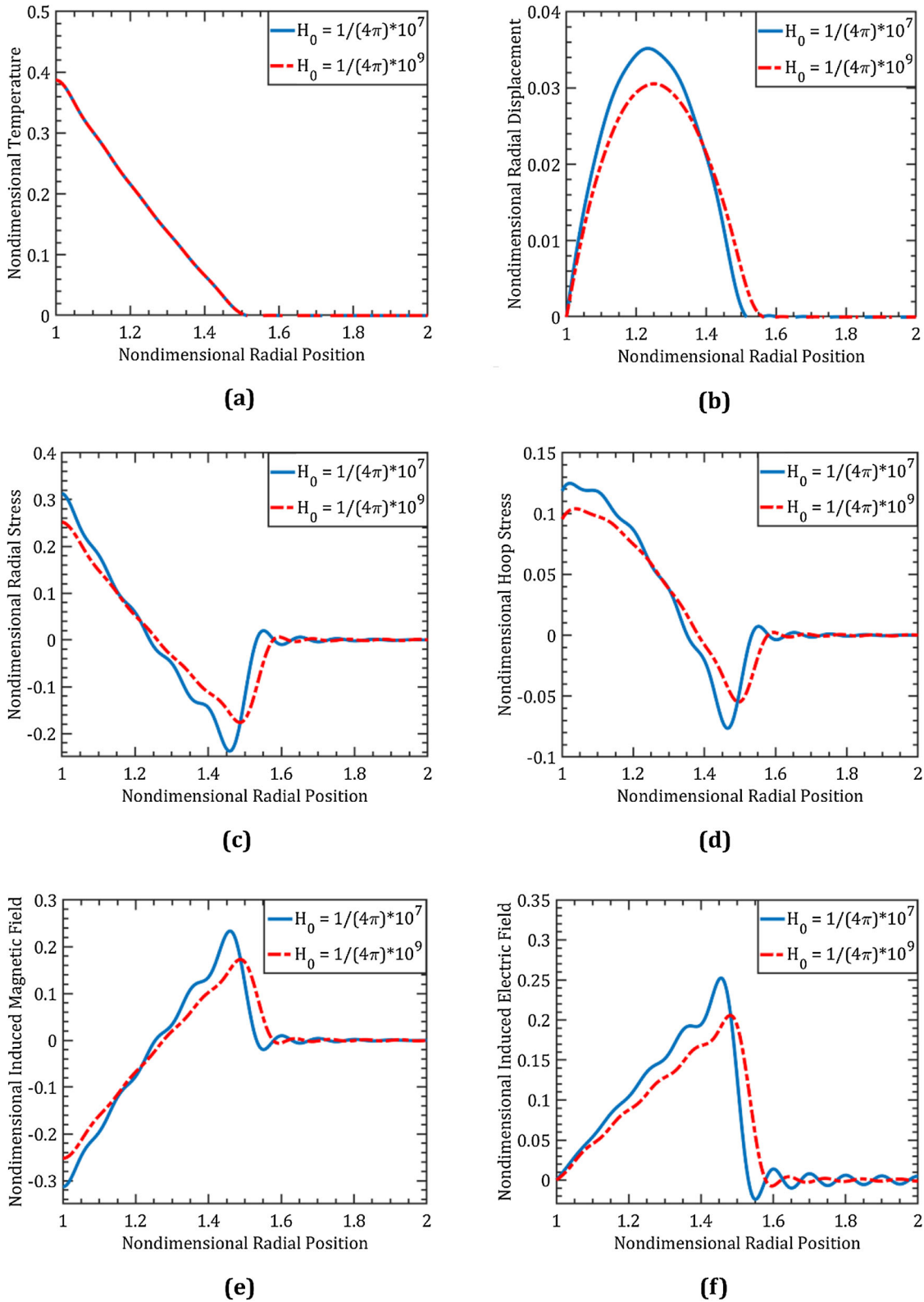
Fig. 3 Through-thickness distribution of nondimensional **a)** temperature **b)** radial displacement **c)** radial stress and **d)** hoop stress **e)** induced magnetic field **f)** induced electric field at $t = 0.5$ for the orthotropic cylinder based on the Lord–Shulman theory. $t_1 = 0, t_2 = t_3 = 1, q_i = 1$
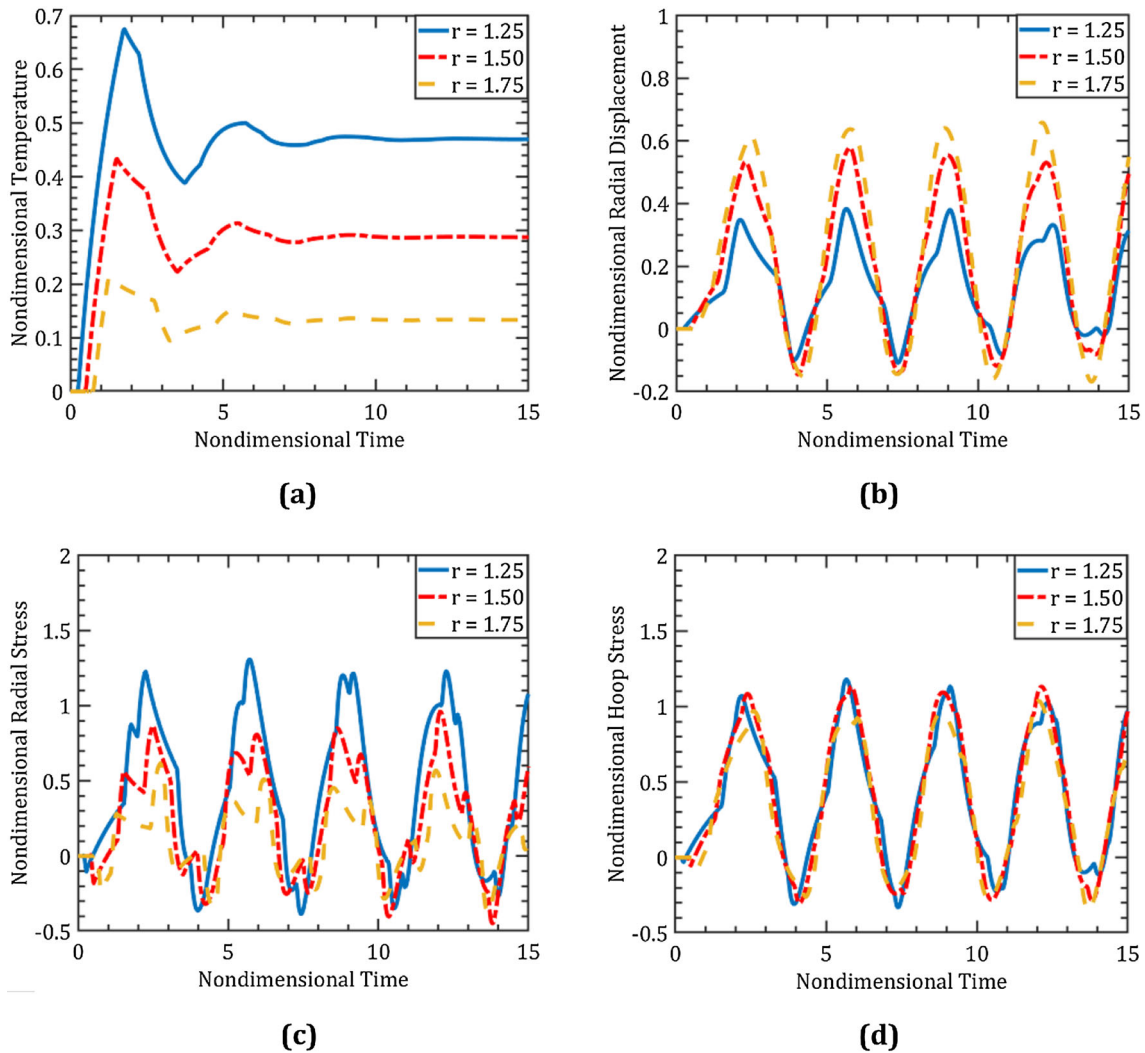
Fig. 4 History of nondimensional **a)** temperature **b)** radial displacement **c)** radial stress and **d)** hoop stress for the orthotropic cylinder based on the Lord–Shulman theory. $t_1 = 0$, $t_2 = t_3 = 1$, $q_i = 1$

(11) and (12), the temperature gradient term exists in both radial and hoop stress components and a steep jump can be seen when the thermal wave reaches any radial position. The effect of boundary conditions on the reflection of the propagated elastic wave is clearly shown in Fig. 6c, d, where the traction-free boundary condition at the outer surface changes the sign of the reflected wave, while the constrained boundary condition at the inner surface reflects the wave with the same sign. As it can be seen in the figures, the radial and hoop stresses are compressive at initial moments and by passing the time both change to the tensile due to the traction-free boundary condition on the outer boundary.

By comparing Figs. 4a and 6a, it can be noted that the histories of the nondimensional temperature are similar for both theories but with different peaks. This difference is due to considering different values for the relaxation times in the Lord–Shulman and Green–Lindsay models. Increasing the value of the relaxation time results in a reduction in the velocity of the temperature wave, which requires more time for the temperature wave to reach its peak point. From the figures, by decreasing the relaxation time from 1.00 to 0.64 (the velocity of thermal wave increases from 1.00 to 1.25), the amplitude of steep jump decreases.

Figure 7 shows through-thickness variation of the nondimensional temperature, displacement, radial and hoop stresses, and induced magnetic and electric fields. The stress wave front at different times can be detected in this figure. As is seen in Fig. 7a, at Time = 0.5 the temperature wave front is at r = 1.625, and the thermoelastic wave front can be observed on Fig. 7b–d. As mentioned earlier, applying the magnetic field
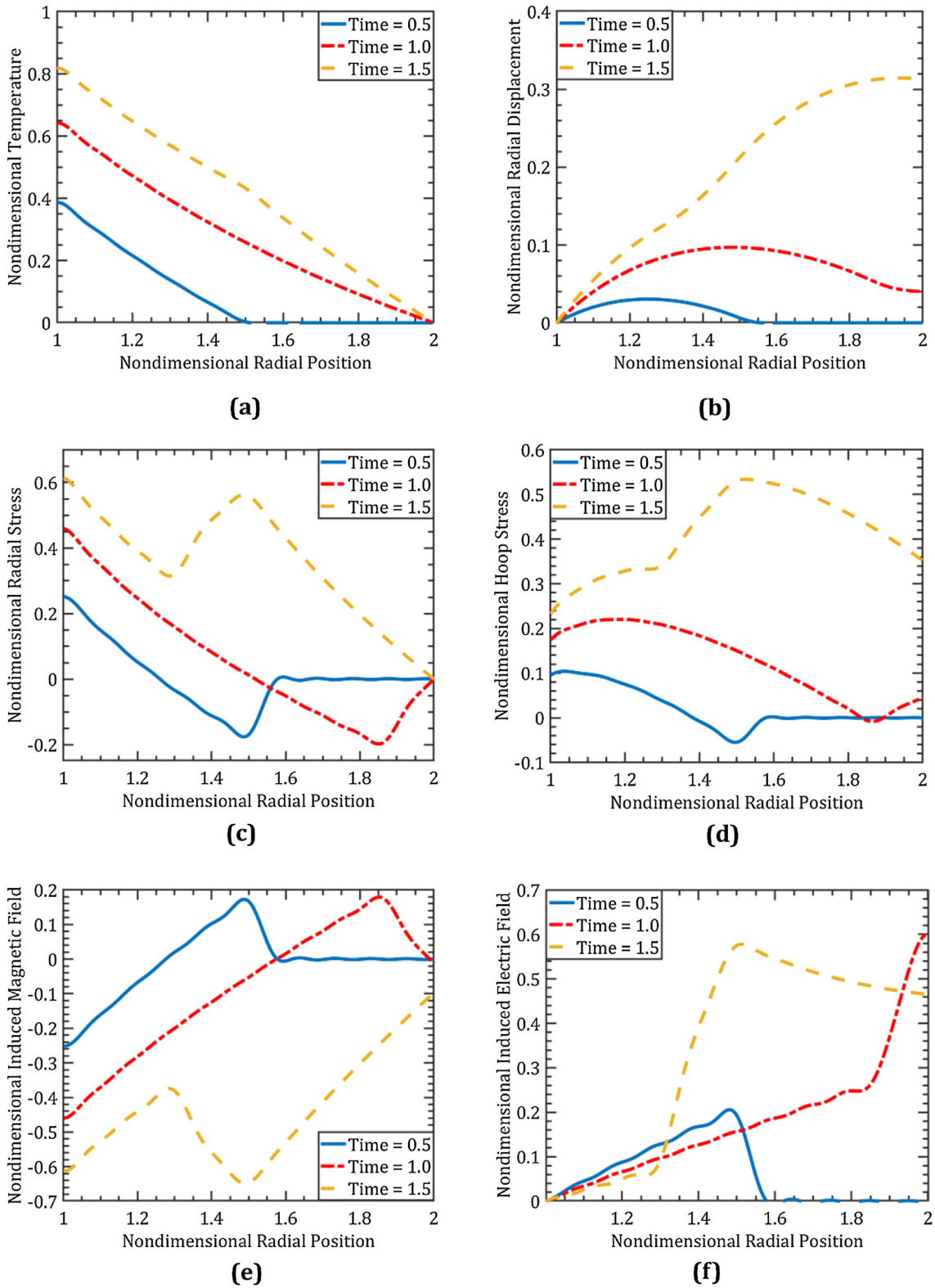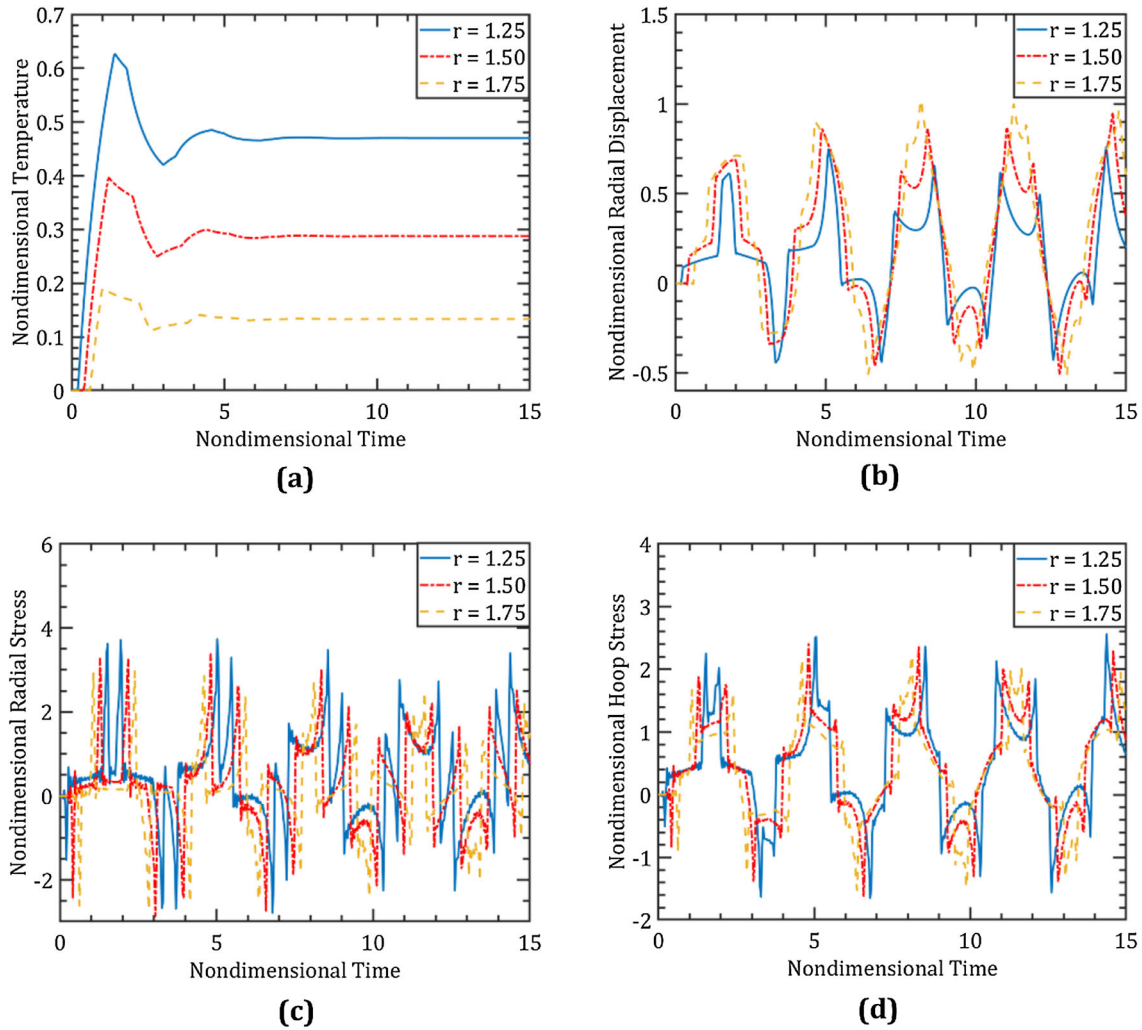
Fig. 5 Through-thickness distribution of nondimensional **a)** temperature **b)** radial displacement **c)** radial stress and **d)** hoop stress **e)** induced magnetic field **f)** induced electric field at different times for the orthotropic cylinder based on the Lord–Shulman theory. $t_1 = 0$, $t_2 = t_3 = 1$, $q_i = 1$

Fig. 6 History of nondimensional **a)** temperature **b)** radial displacement **c)** radial stress and **d)** hoop stress for the orthotropic cylinder based on the Green–Lindsay theory. $t_1 = t_2 = 0.64$, $t_3 = 0$, $q_i = 1$

increases the velocity of the thermoelastic wave propagation to 1.133792, and this moves the positions of steep jumps forward. Similar to the results from the Lord–Shulman theory, the induced magnetic and electric fields exhibit behaviors that parallel the stress wave, and as is seen in Fig. 7, the jumps occur simultaneously at every radial position. Furthermore, the propagation and reflection of the induced magnetic and electric waves can be observed in Fig. 7e, f. While the initiated wave from the inner surface of the cylinder has a negative sign, the waves reflect back into the medium with a positive sign due to the traction-free boundary condition on the outer surface of the cylinder. The time at which the wave front reaches the outer surface of the cylinder for the first time can be calculated as follows:

$$t^* = \frac{b - a}{V_e} = \frac{1}{1.133792} = 0.881995 \tag{154}$$

Figures 8 and 9 illustrate the effect of considering orthotropic material properties on the nondimensional radial and hoop stress components. For the employed material properties in this work $D = 0.9509$. For the isotropic materials, $D = 1$ and leads to the elimination of the sixth term on the left-hand side of the Eq. (34), and consolidation of the last two terms on the left-hand side of the Eq. (33). To exhibit the effect of the considering orthotropic material properties, two different cases were considered. In the first case, $D = 0.9509$ and $\nu = 1.4439$, which is related to the original material properties, and in the second case, $D = 0.4025$ and $\nu = 0.6926$, where all material properties in 1 and 2 directions were exchanged, except for the thermal expansion coefficients.
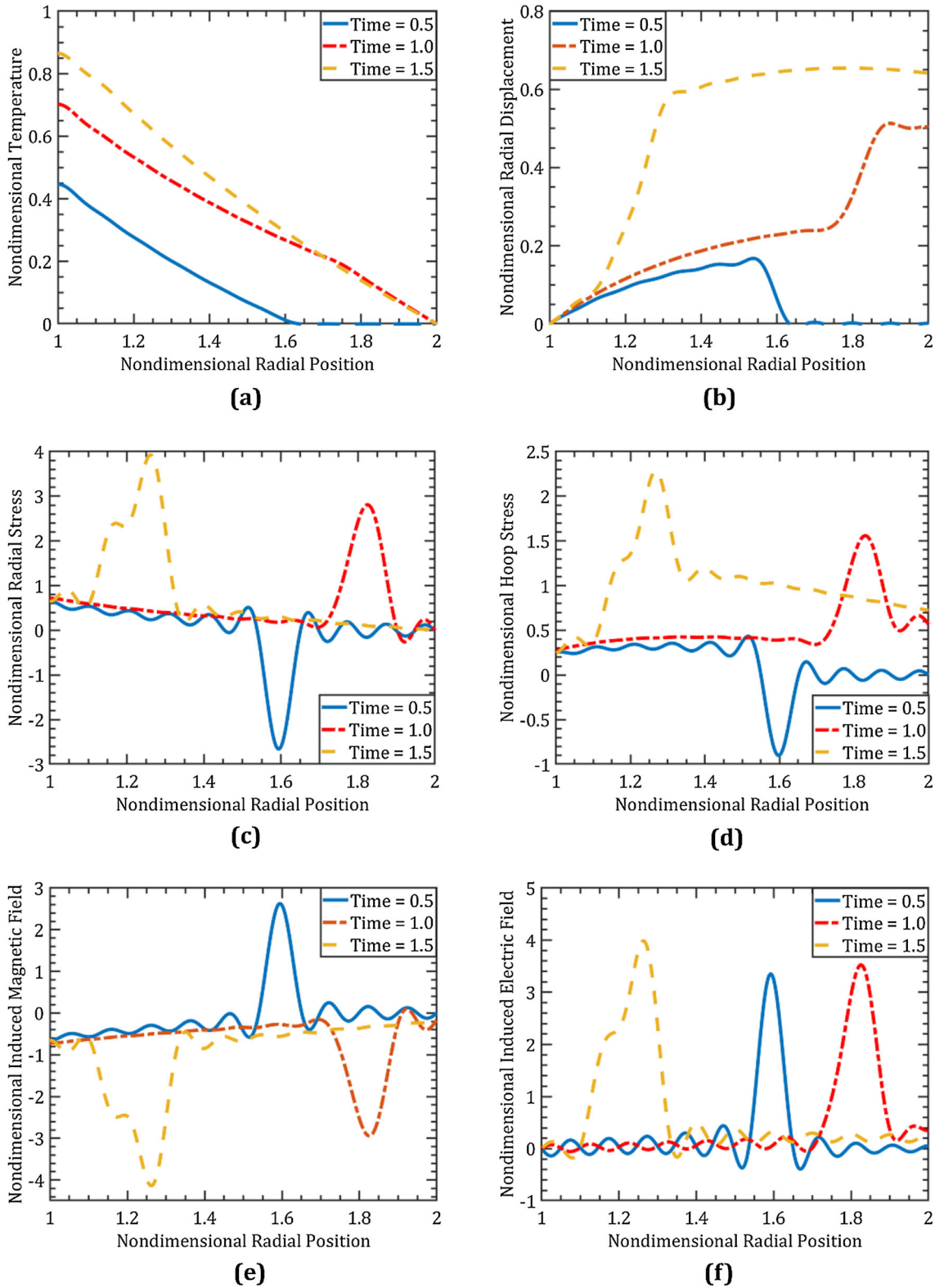
Fig. 7 Through-thickness distribution of nondimensional **a)** temperature **b)** radial displacement **c)** radial stress and **d)** hoop stress **e)** induced magnetic field **f)** induced electric field at different times for the orthotropic cylinder based on the Green–Lindsay theory. $t_1 = t_2 = 0.64$, $t_3 = 0$, $q_i = 1$
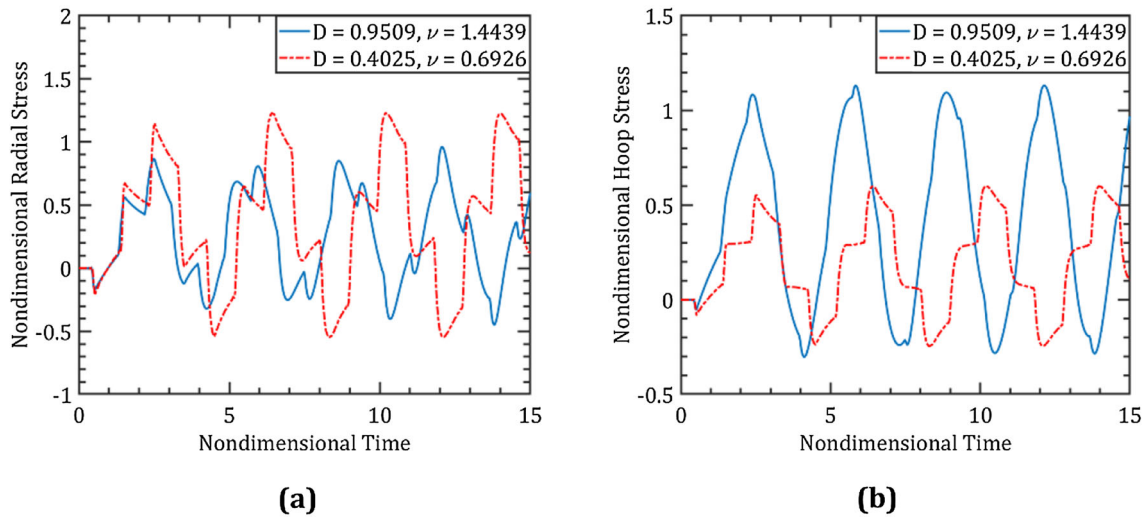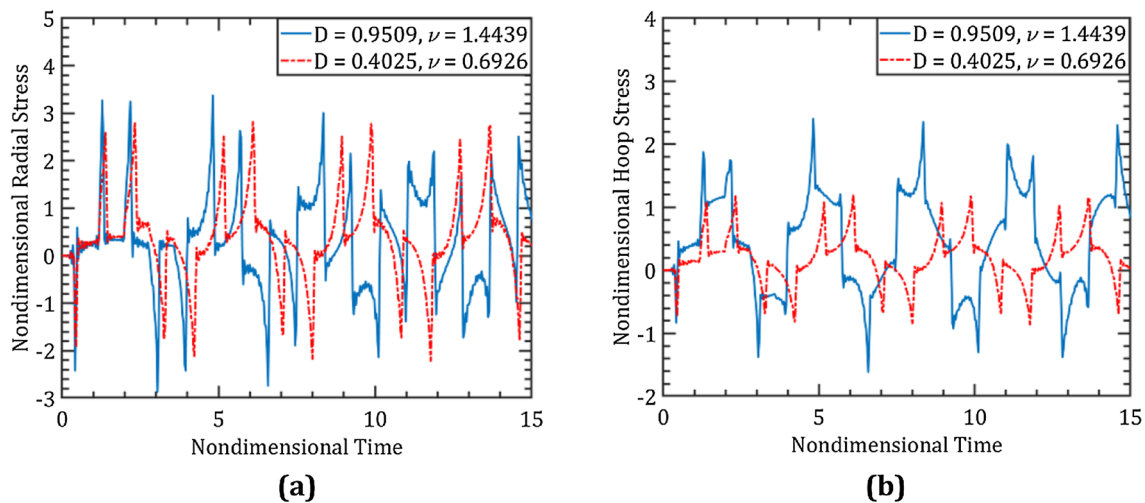
Fig. 8 History of nondimensional **a)** radial stress and **b)** hoop stress at the mid-radius of the orthotropic cylinder the Lord–Shulman theory. $t_1 = 0$, $t_2 = t_3 = 1$, $q_i = 1$

Fig. 9 History of nondimensional **a)** radial stress and **b)** hoop stress at the mid-radius of the orthotropic cylinder based on the Green–Lindsay theory. $t_1 = t_2 = 0.64$, $t_3 = 0$, $q_i = 1$

As is depicted in the Fig. 8a, b, decreasing the D and ν coefficients leads to an increase in the radial stress and a decrease in the hoop stress, which is expected when material properties in r and θ were exchanged. Figure 9 shows the results for the mentioned cases based on the Green–Lindsay theory. While similar changes can be observed in Fig. 9b, in Fig. 9a, the amplitude of the radial stress does not change considerably, which can be attributed to the significant impact of the rate of temperature change over time in the Green–Lindsay theory.

5 Conclusion

In this paper, the equations of generalized coupled magneto–thermoelasticity problem in an orthotropic hollow cylinder, based on the Lord–Shulman and Green–Lindsay theories, were presented and solved using analytical methods. The cylinder was subjected to a thermal shock in the form of a heat flux on its inner surface and a constant temperature on the outer surface. The mechanical boundary conditions of the problem for the outer and inner surfaces of the cylinder were the traction-free and constrained, respectively. Additionally, a constant magnetic field in the form of a body force was applied to the orthotropic cylinder. Following the presentation

of a closed-form solution for the problem, the effects of the amplitude of the applied magnetic field on the distribution of temperature, displacement, stress components and induced magnetic and electric fields were illustrated in figures. The effects of considering orthotropic material properties for the cylinder on the history of the radial stress and hoop stress components were demonstrated in the figures. To validate the results of the presented solution, the problem of generalized thermoelasticity based on the Lord–Shulman theory in a disk subjected to a thermal shock, was considered, and the results were compared with those obtained by Kiani and Eslami [34], where a significant consistency was noted.

Declarations

Conflict of interest The authors have no relevant financial or non-financial interests to disclose.

References

1. Somireddy, M., Czekanski, A.: Anisotropic material behavior of 3D printed composite structures—material extrusion additive manufacturing. Mater. Des. **195**, 108953 (2020). https://doi.org/10.1016/j.matdes.2020.108953
2. Chen, H.-T., Lin, H.-J.: Study of transient coupled thermoelastic problems with relaxation times. J. Appl. Mech. **62**, 208–215 (1995). https://doi.org/10.1115/1.2895904
3. Hetnarski, R.B., Eslami, M.R., Gladwell, G.M.L.: Thermal Stresses: Advanced Theory and Applications. Springer, Berlin (2009)
4. Guha, S., Singh, A.K., Singh, S.: Thermoelastic damping and frequency shift of different micro-scale piezoelectro–magneto–thermoelastic beams. Phys. Scr. **99**, 15203 (2023). https://doi.org/10.1088/1402-4896/ad0bbd
5. Sherief, H.H., Ezzat, M.A.: A problem in generalized magneto–thermoelasticity for an infinitely long annular cylinder. J. Eng. Math. **34**, 387–402 (1998). https://doi.org/10.1023/A:1004376014083
6. Zenkour, A.M., Abbas, I.A.: Magneto–thermoelastic response of an infinite functionally graded cylinder using the finite element method. J. Vib. Control **20**, 1907–1919 (2014). https://doi.org/10.1177/1077546313480541
7. Hosseini, M., Dini, A.: Magneto-thermo-elastic response of a rotating functionally graded cylinder. Struct. Eng. Mech. Int. J. **56**, 137–156 (2015)
8. Abd-El-Salam, M.R., Abd-Alla, A.M., Hosham, H.A.: A numerical solution of magneto–thermoelastic problem in non-homogeneous isotropic cylinder by the finite-difference method. Appl. Math. Model. **31**, 1662–1670 (2007). https://doi.org/10.1016/j.apm.2006.05.009
9. Das, P., Kar, A., Kanoria, M.: Analysis of magneto–thermoelastic response in a transversely isotropic hollow cylinder under thermal shock with three-phase-lag effect. J. Therm. Stress **36**, 239–258 (2013). https://doi.org/10.1080/01495739.2013.765180
10. Abbas, I.A.: Generalized magneto–thermoelasticity in a nonhomogeneous isotropic hollow cylinder using the finite element method. Arch. Appl. Mech. **79**, 41–50 (2009). https://doi.org/10.1007/s00419-009-0301-6
11. Abbas, I.A.: Generalized magneto–thermoelastic interaction in a fiber-reinforced anisotropic hollow cylinder. Int. J. Thermophys. **33**, 567–579 (2012). https://doi.org/10.1007/s10765-012-1178-0
12. Abd-Alla, A.M., Mahmoud, S.R.: Magneto–thermoelastic problem in rotating non-homogeneous orthotropic hollow cylinder under the hyperbolic heat conduction model. Meccanica **45**, 451–462 (2010). https://doi.org/10.1007/s11012-009-9261-8
13. Biswas, S.: Eigenvalue approach to a magneto–thermoelastic problem in transversely isotropic hollow cylinder: comparison of three theories. Waves Random Complex Media **31**, 403–419 (2021). https://doi.org/10.1080/17455030.2019.1588484
14. Othman, M.I.A., Abbas, I.A.: Effect of rotation on magneto–thermoelastic homogeneous isotropic hollow cylinder with energy dissipation using finite element method. J. Comput. Theor. Nanosci. **12**, 2399–2404 (2015). https://doi.org/10.1166/jctn.2015.4039
15. Said, S.M., Abd-Elaziz, E.M., Othman, M.I.A.: A two-temperature model and fractional order derivative in a rotating thick hollow cylinder with the magnetic field. Indian J. Phys. **97**, 3057–3064 (2023). https://doi.org/10.1007/s12648-023-02651-w
16. Ezzat, M.A., El-Bary, A.A.: Effects of variable thermal conductivity and fractional order of heat transfer on a perfect conducting infinitely long hollow cylinder. Int. J. Therm. Sci. **108**, 62–69 (2016). https://doi.org/10.1016/j.ijthermalsci.2016.04.020
17. Sherief, H.H., Allam, A.A.: Electro–magneto interaction in a two-dimensional generalized thermoelastic solid cylinder. Acta Mech. **228**, 2041–2062 (2017). https://doi.org/10.1007/s00707-017-1814-7
18. Patra, S., Shit, G.C., Das, B.: Computational model on magnetothermoelastic analysis of a rotating cylinder using finite difference method. Waves Random Complex Media **32**, 1654–1671 (2022). https://doi.org/10.1080/17455030.2020.1831710
19. Akbarzadeh, A., Chen, Z.: Thermo-magneto-electro-elastic responses of rotating hollow cylinders. Mech. Adv. Mater. Struct. **21**, 67–80 (2014). https://doi.org/10.1080/15376494.2012.677108
20. Othman, M.I.A.: Relaxation effects on thermal shock problems in an elastic half-space of generalized magneto–thermoelastic waves. Mech. Mech. Eng. **7**, 165–178 (2004)
21. Othman, M.I.A.: Generalized electromagneto–thermoelastic plane waves by thermal shock problem in a finite conductivity half-space with one relaxation time. Multidiscip. Model. Mater. Struct. **1**, 231–250 (2005). https://doi.org/10.1163/157361105774538557

22. Othman, M.I.A.: Generalized electromagneto-thermoviscoelastic in case of 2-D thermal shock problem in a finite conducting medium with one relaxation time. Acta Mech. **169**, 37–51 (2004). https://doi.org/10.1007/s00707-004-0101-6
23. Othman, M.I.A., Abd-Elaziz, E.M.: Effect of rotation on a micropolar magneto–thermoelastic solid in dual-phase-lag model under the gravitational field. Microsyst. Technol. **23**, 4979–4987 (2017). https://doi.org/10.1007/s00542-017-3295-y
24. Othman, M.I.A., Hasona, W.M., Eraki, E.E.M.: Effect of magnetic field on generalized thermoelastic rotating medium with two temperature under five theories. J. Comput. Theor. Nanosci. **12**, 1677–1686 (2015). https://doi.org/10.1166/jctn.2015.3946
25. Shahani, A.R., Sharifi Torki, H.: Analytical solution of the thermoelasticity problem in a thick-walled cylinder subjected to transient thermal loading. Modares Mech. Eng. **16**, 147–154 (2017)
26. Shahani, A.R., Sharifi Torki, H.: Determination of the thermal stress wave propagation in orthotropic hollow cylinder based on classical theory of thermoelasticity. Contin. Mech. Thermodyn. **30**, 509–527 (2018). https://doi.org/10.1007/s00161-017-0618-2
27. Sharifi Torki, H., Shahani, A.R.: Analytical solution of the coupled dynamic thermoelasticity problem in a hollow cylinder. J. Stress Anal. **5**, 121–134 (2020). https://doi.org/10.22084/JRSTAN.2020.22464.1155
28. Sharifi, H.: Analytical solution for thermoelastic stress wave propagation in an orthotropic hollow cylinder. Eur. J. Comput. Mech. **31**, 239–274 (2022). https://doi.org/10.13052/ejcm2642-2085.3124
29. Jabbari, M., Mohazzab, A.H., Bahtui, A., Eslami, M.R.: Analytical solution for three-dimensional stresses in a short length FGM hollow cylinder. ZAMM J. Appl. Math. Mech. für Angew Math. und Mech. Appl. Math. Mech. **87**, 413–429 (2007). https://doi.org/10.1002/zamm.200610325
30. Jabbari, M., Dehbani, H., Eslami, M.R.: An exact solution for classic coupled thermoelasticity in cylindrical coordinates. J. Press. Vessel. Technol. **133**, 051204 (2011). https://doi.org/10.1115/1.4003459
31. Bagri, A., Eslami, M.R.: Generalized coupled thermoelasticity of disks based on the Lord–Shulman model. J. Therm. Stress **27**, 691–704 (2004). https://doi.org/10.1080/01495730490440127
32. Bagri, A., Eslami, M.R.: Generalized coupled thermoelasticity of functionally graded annular disk considering the Lord–Shulman theory. Compos. Struct. **83**, 168–179 (2008). https://doi.org/10.1016/j.compstruct.2007.04.024
33. Sharifi, H.: Generalized coupled thermoelasticity in an orthotropic rotating disk subjected to thermal shock. J. Therm. Stress **45**, 695–719 (2022). https://doi.org/10.1080/01495739.2022.2091066
34. Kiani, Y., Eslami, M.R.: A GDQ approach to thermally nonlinear generalized thermoelasticity of disks. J. Therm. Stress **40**, 121–133 (2017). https://doi.org/10.1080/01495739.2016.1217179
35. Kiani, Y., Karimi Zeverdejani, P.: Thermally nonlinear response of an exponentially graded disk using the Lord–Shulman model. J. Therm. Stress **43**, 1547–1563 (2020). https://doi.org/10.1080/01495739.2020.1810186
36. Tokovyy, Y., Chyzh, A., Ma, C.-C.: An analytical solution to the axisymmetric thermoelasticity problem for a cylinder with arbitrarily varying thermomechanical properties. Acta Mech. **230**, 1469–1485 (2019). https://doi.org/10.1007/s00707-017-2012-3
37. Bagri, A., Eslami, M.R.: A unified generalized thermoelasticity; solution for cylinders and spheres. Int. J. Mech. Sci. **49**, 1325–1335 (2007). https://doi.org/10.1016/j.ijmecsci.2007.04.004
38. Sharifi, H.: Dynamic response of an orthotropic hollow cylinder under thermal shock based on Green–Lindsay theory. Thin Walled Struct. **182**, 110221 (2023). https://doi.org/10.1016/j.tws.2022.110221
39. Soroush, M., Soroush, M.: Thermal stresses in an orthotropic hollow sphere under thermal shock: a unified generalized thermoelasticity. J. Eng. Math. **145**, 1–34 (2024). https://doi.org/10.1007/s10665-023-10321-3
40. Othman, M.I.A., Abbas, I.A.: Generalized thermoelasticity of thermal-shock problem in a non-homogeneous isotropic hollow cylinder with energy dissipation. Int. J. Thermophys. **33**, 913–923 (2012). https://doi.org/10.1007/s10765-012-1202-4
41. Tiwari, R., Abouelregal, A.E.: Thermo-viscoelastic transversely isotropic rotating hollow cylinder based on three-phase lag thermoelastic model and fractional Kelvin–Voigt type. Acta Mech. **233**, 2453–2470 (2022). https://doi.org/10.1007/s00707-022-03234-2
42. Marin, M., Hobiny, A., Abbas, I.: The effects of fractional time derivatives in porothermoelastic materials using finite element method. Mathematics **9**, 1606 (2021). https://doi.org/10.3390/math9141606
43. Marin, M., Seadawy, A., Vlase, S., Chirila, A.: On mixed problem in thermoelasticity of type III for Cosserat media. J. Taibah Univ. Sci. **16**, 1264–1274 (2022). https://doi.org/10.1080/16583655.2022.2160290
44. Decolon, C.: Analysis of Composite Structures. Elsevier, Amsterdam (2004)
45. Abbas, I.A., Abd-Alla, A.-E.-N.N.: Effects of thermal relaxations on thermoelastic interactions in an infinite orthotropic elastic medium with a cylindrical cavity. Arch. Appl. Mech. **78**, 283–293 (2008). https://doi.org/10.1007/s00419-007-0156-7
46. Karimipour Dehkordi, M., Kiani, Y.: Lord–Shulman and Green–Lindsay-based magneto–thermoelasticity of hollow cylinder. Acta Mech. **235**, 51–72 (2023). https://doi.org/10.1007/s00707-023-03739-4
47. Shahani, A.R., Bashusqeh, S.M.: Analytical solution of the coupled thermo-elasticity problem in a pressurized sphere. J. Therm. Stress **36**, 1283–1307 (2013). https://doi.org/10.1080/01495739.2013.818889
48. Cinelli, G.: An extension of the finite Hankel transform and applications. Int. J. Eng. Sci. **3**, 539–559 (1965). https://doi.org/10.1016/0020-7225(65)90034-0
49. Sneddon, I.N.: The Use of Integral Transforms. McGraw-Hill, New York (1972)